ORIGINAL ARTICLE

Investigation of hydrogeological conditions of a fractured shale aquifer in Yala Area (SE Nigeria) characterized by saline groundwater

Aniekan Edet[1] · Chiedu Okereke[1]

Abstract

Geological, hydrogeological and geophysical investigations were carried out in Yala Area (SE Nigeria) to delineate potential zones for future groundwater development. The area is underlain by Turonian fractured shale rock intruded by basaltic rocks and saline water. High lineament density (> 30 km^{-1}) recorded in the north suggest high permeable zone, compared with low lineament density (< 10 km^{-1}) in the south and east. Geophysical results reveal four types of aquifers: an upper weathered, fractured shale aquifer with mean resistivity and thickness in the range 27–40 Ω m and 20–28 m and a lower fractured shale aquifer with mean resistivity in the range 28.5 to 36.0 Ω m and unresolved thickness; fractured saline shale aquifer with mean resistivity and thickness of 21 Ω m and 50 m; fractured silty shale aquifer with mean resistivity and thickness of 54.4 Ω m and 10 m and basaltic intrusive fractured shale aquifer with mean resistivity and thickness of 135.6 Ω m and 6 m. A broad range of aquifer parameters were obtained from resistivity data and pumping test. Groundwater quality on the mean indicated alkaline and good fresh water for drinking and irrigation use with minor level of salinization. Concentration of dissolved ions in the area are enhanced through weathering and ion exchange. On the basis of these data, the potential zones for groundwater harnessing have been delineated in Yala Area.

Keywords Fractured shale · Groundwater development · Lineament · Resistivity · Water quality · Nigeria

Introduction

Fractured shale aquifers cover Yala Area, southeastern Nigeria and groundwater stored in these fractures, over the years has been a source of potable water to support food and livelihood security. However, the area experiences water scarcity due to low permeability rock, low rainfall, decrease in surface water and saline water intrusion. Scarcity of water is very serious in the dry season as a result of which the local people walk for some distance to obtain potable water or in some cases make do with polluted surface water. To date, few, but not comprehensive studies on the groundwater potentials of Yala Area including the surrounding areas have been recorded in literature. Most of the researches were on the aquifer delineation using vertical electrical soundings (VES), origin, occurrence and quality of saline groundwater mainly within the

surroundings of Yala. Studies in similar terrain near the present study area showed that MacDonald et al. (2001) applied an integrated geophysical technique that involved frequency domain EM conductivity, vertical electrical resistivity soundings (VES) and magnetic profiling to identify groundwater targets in low permeability shales, siltstones, sandstones and basic intrusive igneous rocks in Oju southeastern Nigeria. The study identified three areas of groundwater interest: sandy units within shales; fractured zones within shales and fractures associated with shales. In addition, Eke and Igboekwe (2011) used 20 VES data to identify good groundwater potentials in Ohafia shale area, while Umeh et al. (2014), working in the shale-clay-sand area of Lokpaukwu, identified potential groundwater areas from VES measurements. However, these results were not evaluated through drilling. In order to contribute to groundwater development in the Abakaliki shale area due to frequent borehole failure, Aghamelu et al. (2013) used VES data to identify six hydrogeolectric layers. The study, however, failed to identify any aquifer, rather suggested further work using an integrated geophysical survey for identification of productive borehole

✉ Aniekan Edet
aniekanedet@yahoo.com

1   Department of Geology, University of Calabar, Calabar, Nigeria

areas. Agha (2015) working within the same Abakaliki shale area, interpreted 5 layers from VESs and identified a layer composed of splintery saturated shale as potential aquifer. Okonkwo et al (2016) used 78 VES data in Agwu Shale area, while Okamkpa et al (2018) used 12 VES data within Enugu Shale area to identify groundwater potential areas. Recently, Onwe et al. (2019) applied VES data from 15 locations to study the groundwater situation in shale area of Ebonyi North. The study showed that weathered and fractured shale layers constituted the productive water bearing zone. Within Yala Area, Mbipom et al. (1990) applied seismic refraction and VES measurements at Okpoma (designated as UK 45 in this study) to delineate zones of high salinity at depths of between 20 and 244 m below the ground surface. Ushie and Nwankwoala (2011) used 24 VESs to identified two groundwater potentials zones. The research of Akiang et al. (2020) in Abakpa in Ogoja, northeast of Yala revealed three to seven geoelectric layers and distinguished saline and brackish groundwater from fresh groundwater units at depths of 7.8–56.9 m. The VES results were however, not supported by drilling for evaluation purposes. Also no chemical data confirm the salinity level of groundwater from existing boreholes in the area.

Some of the earlier studies on hydrochemical assessment showed that Uma and Onuoha (1990) identified two hydrogeologic groups within the Lower Benue Trough (Nigeria), where YLGA is located, while Uma et al. (1990) noted that the occurrences of saline water are not randomly distributed, but influenced by the orientation of the dominant tectonic features. Ekwere and Ukpong (1994) used chemical composition of dissolved salts to characterize the origin of saltwater in Ogoja, located southwest of Yala. The study concluded that high concentrations of Na^+, K^+, Ca^{2+}, Mg^{2+} and Cl^- suggested marine rather than continental origin for the brines. Tijani et al (1996) used a combination of stratigraphic setting, hydrochemical and isotopic data to show that the brines in Ogoja area are of marine origin related to paleo seawater embedded within the sediments. In other parts of the world with similar saline groundwater problems, Choudhury et al. (2001) employed geophysical techniques to investigate the occurrence of saline contaminated aquifer. The study also delineated different hydrogeological related formations using resistivity data and demarcated safe zones where groundwater could be exploited. Balia et al (2009) used hydrogeological and geophysical means to delineate complex aquifer system, differentiate structures and elucidated seawater affecting aquifers. Above examples have shown the contributions and success of geophysical data to evaluate the potentials of groundwater in a fractured shale terrain characterized with saline ponds and groundwater. However, these studies used mainly VES without geological, hydrogelogical and hydrochemical controls. Besides,

these studies did not take into consideration the occurrence of saline groundwater, despite the fact it exist in the areas studied.

Shale rocks exhibit low or no primary porosity and permeability, hence occurrence and movement of groundwater is enhanced through fractured porosity and permeability developed through weathering and fracturing (Edet 1993a; MacDonald et al. 2001). Since the shale aquifer in YLGA area is characterized by low storage and yield of groundwater, hence, there is the need to characterize its hydrogeological setting. This study was therefore undertaken to delineate the aquifer geometry, its characteristics, distribution of water table and assess the quality of water and sources of ions. Hence, various approaches were applied to investigate the potentials of the underlying fractured shale bedrock for groundwater exploration and sustainable development.

Location, physiography, geology and hydrogeology

The Yala study area is situated between latitudes $6°15'–6°56'$ N and longitudes $8°20'–8°50'$ E. The terrain is gently undulating with dotting of isolated hills, with a mean elevation of about 45 m above mean sea level (amsl). Meteorological data in 2009 for nearby Ogoja station (Fig. 1), show air temperature in the range 31.4 to 37.5 °C (mean 33.7 °C). Precipitation in form of rainfall varies between 0 and 454.7 mm with a monthly mean of 228.2 mm. Relative humidity averaged 77.2%, ranging between 58 and 89%.

The study area is located within the Nigerian Benue Trough. The Benue Trough is over 800 km long and 100–150 km wide, striking northeast rift-like basin that formed during the initial splitting of the African and South American Continents which formed the Atlantic Ocean (McDonald et al 2001; Tijani et al 1996). The Benue Trough is filled with more than 3000 m of folded marine and fluviatile sediments (Benkhhelil 1989), which have been affected by two sets of tectonism, in pre Turonian and Santonian Times (Uma and Löhnert 1992) Specifically, Yala lies within the Lower Benue Trough in Ogoja Syncline, where the main formation is the Eze Aku Formation is composed of fractured shales with intercalations of sandstones. The Eze Aku Formation is underlain by the Asu River Group (Fig. 1). The Asu River Group comprises bluish black shales with minor sandstone units. The shales are fractured and associated with pyroclastic rocks (Hoque 1984; Uma and Onuoha 1990) and basaltic rocks. These basaltic rocks were encountered in the field and from lithologic logs (Edet, 1993a; Okereke et al. 1998).

Yala Area falls into the first hydrogeological group of the Lower Benue Trough (Uma and Onuoha 1990). The major feature of the group is the occurrence of thin shallow unconfined
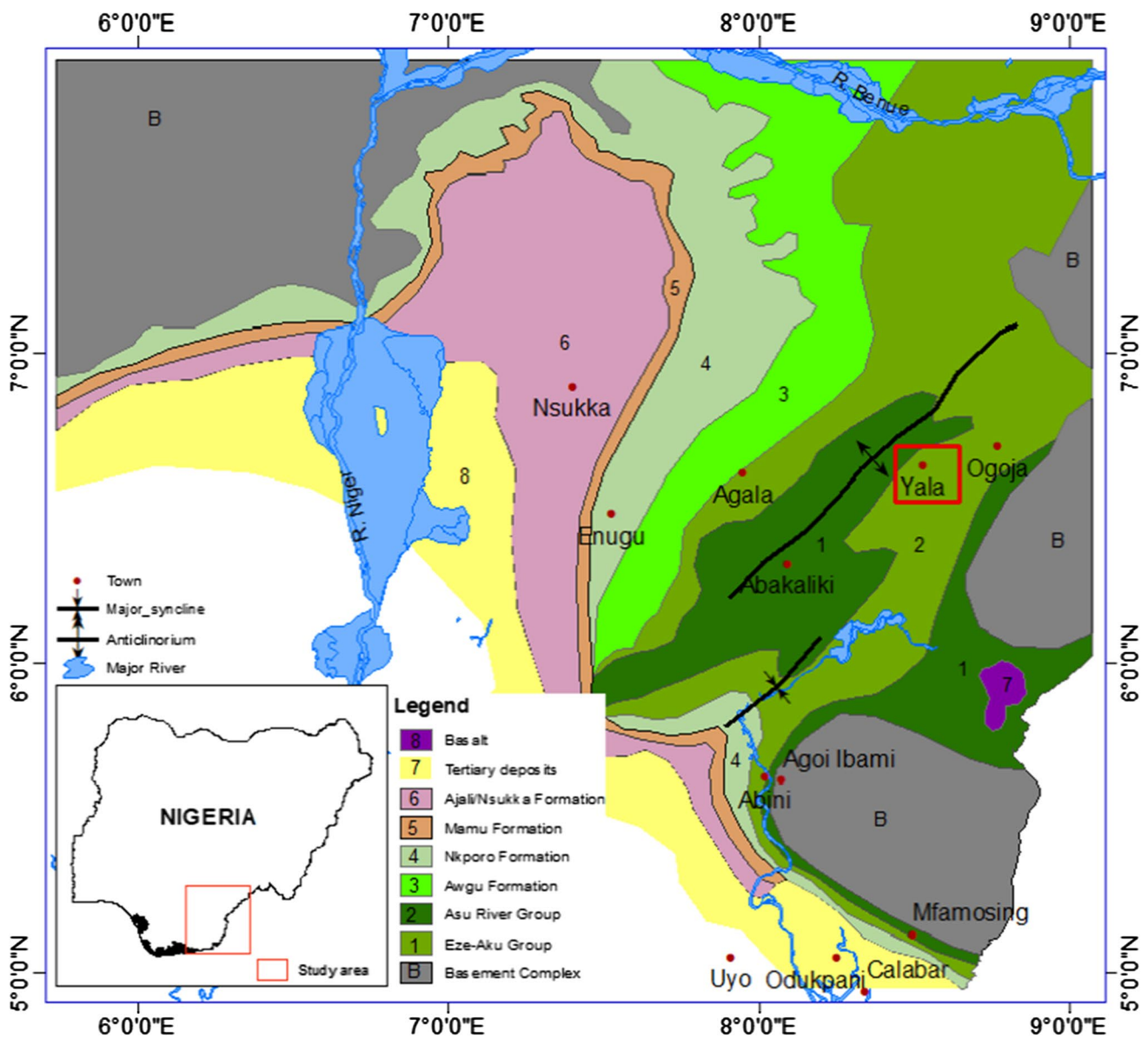
Fig. 1 Geological map of parts of southern Benue trough, Nigeria including the study area

aquifer. Groundwater here exist in three different types of environments (McDonald et al 2001). The main targets include top weathered shale horizon in continuity with fractured shales, sandstone horizons and basaltic intrusive (Fig. 2). The top weathered shale zone is highly permeable and sustain shallow hand dug wells. The depth to the water table is generally < 20 m (Uma and Onuoha 1990) with average of 4.2 m and yield of 20 m^3/d and 200 m^3/d for the shale and sandstone horizons (Ekwere and Ukpong 1994). Open fractures are common within the Asu River Group and Eze Aku Shales. These fractures have been attributed to unloading and

enhanced by dissolution. Pumping test located in the fractured zones indicate transmissivity values in the range 0.5 to 5.0 m^2/d. Sandstones are intercalated within the shales of Eze Aku Formation. The sandstone can support deep hand dug wells. Transmissivity estimates of the sandstone are generally < 0.3 m^2/d. Basaltic intrusive and baked shale areas constitutes the main target for groundwater in some areas. Transmissivity in this basaltic area is in excess of 30 m^2/d. This is possible in areas with negligible potential for groundwater from sediments, which are too soft for fractures to remain open. (McDonald et al 2001).
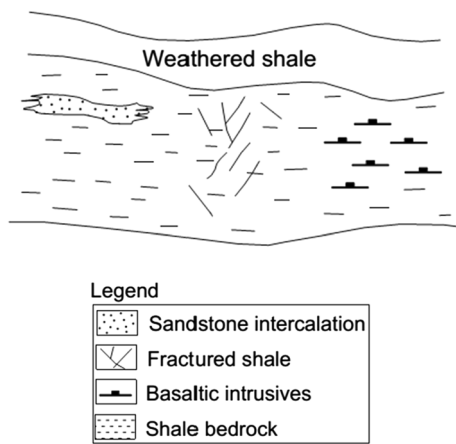
Materials and methods

The study involved field survey, lineament mapping, surface resistivity, geological, hydrogeological and hydrochemical data gathering to unraveled the hydrogeological conditions of Yala.

Geological and hydrogeological data

Groundwater geologic map on a scale 1:250,000 (CRBDA, 1982) was used to produce lineament map for the area according to the techniques outlined in Greenbaum (1985), Edet (1993a) and Edet and Okereke (2005) as presented below:
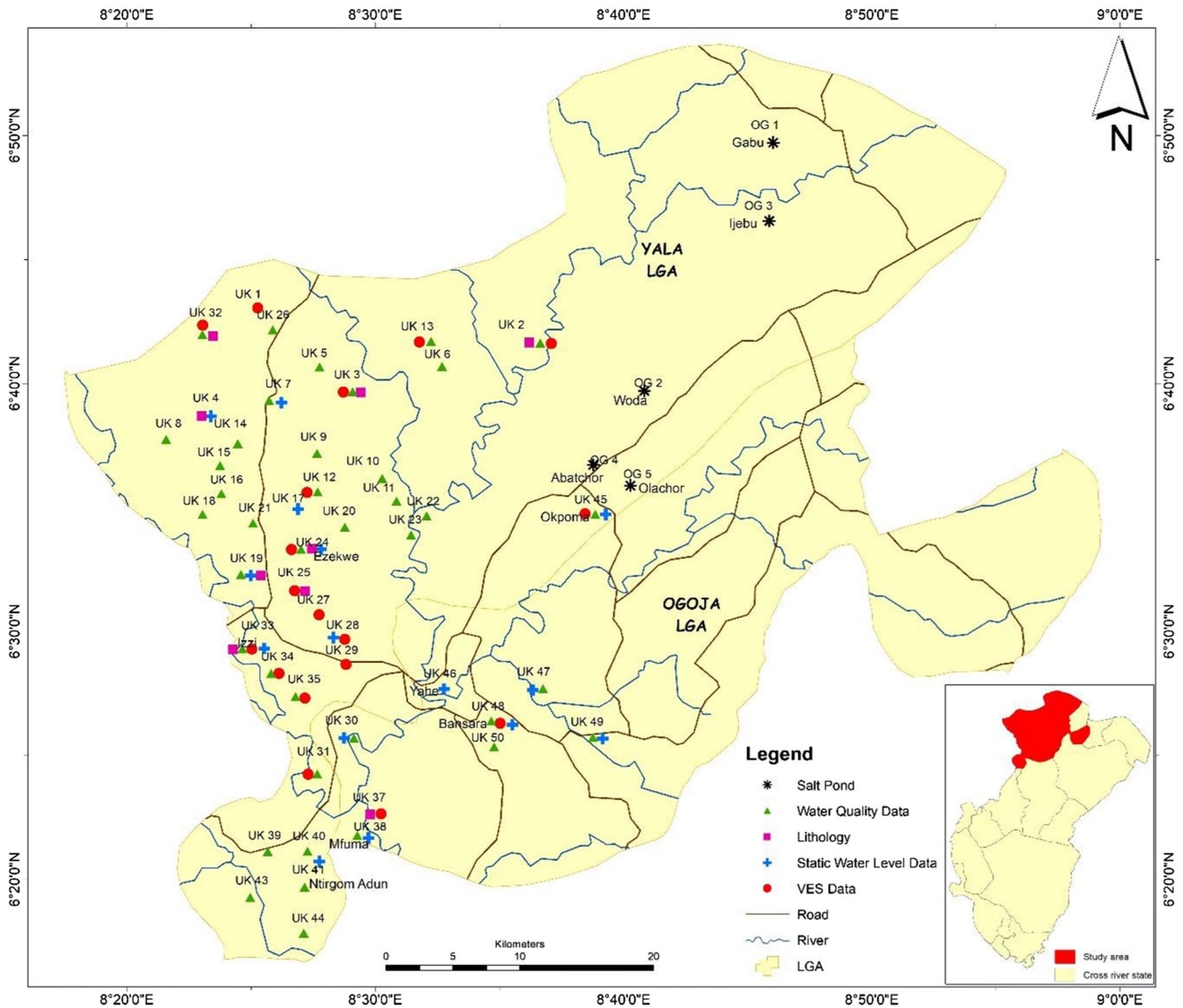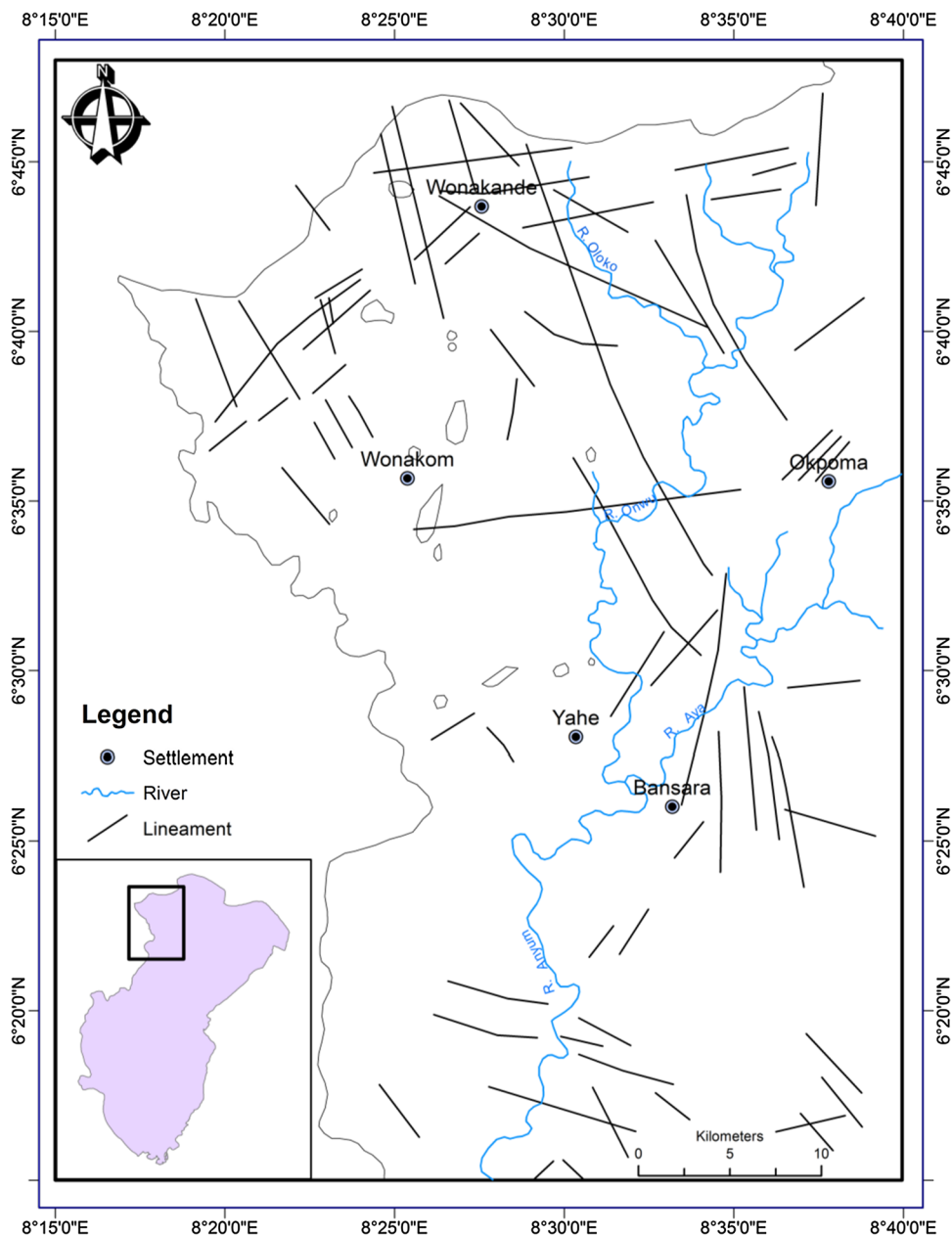

Fig. 2 Schematic diagram of the main groundwater targets in Yala area (Modified from MacDonaldet al. 2001)

Fig. 3 Map of Yala Area with VES, water quality and lithology data locations

Fig. 4 Lineament map of Yala Area

$$LD = \frac{\sum_{i=1}^{i=n} L_i}{A} \qquad (1)$$

where LD is lineament density (m^{-1}), L_i length of individual lineament (m), and A areal coverage (m^2).

Hydrogeological studies performed include measurements of static water levels from wells and boreholes, use of secondary data such as lithologic description from boreholes/well logs, pumping test data, static water levels and borehole/well depths from water development agencies to delineate aquifer geometry and their properties and groundwater sampling for determination of physicochemical parameters, sources of ions and quality assessment.

Static water level fluctuations were monitored at two locations, one within and one outside Yala area, between March and November 2008.

Geophysical data and estimation of aquifer parameters

Vertical electrical sounding (VES) survey was made with an ABEM Terrameter SAS 300 employing the Schlumberger configuration. In the survey, direct current was sent into the ground through a pair of current electrodes (A, B) and another pair of potential electrodes (M, N) which
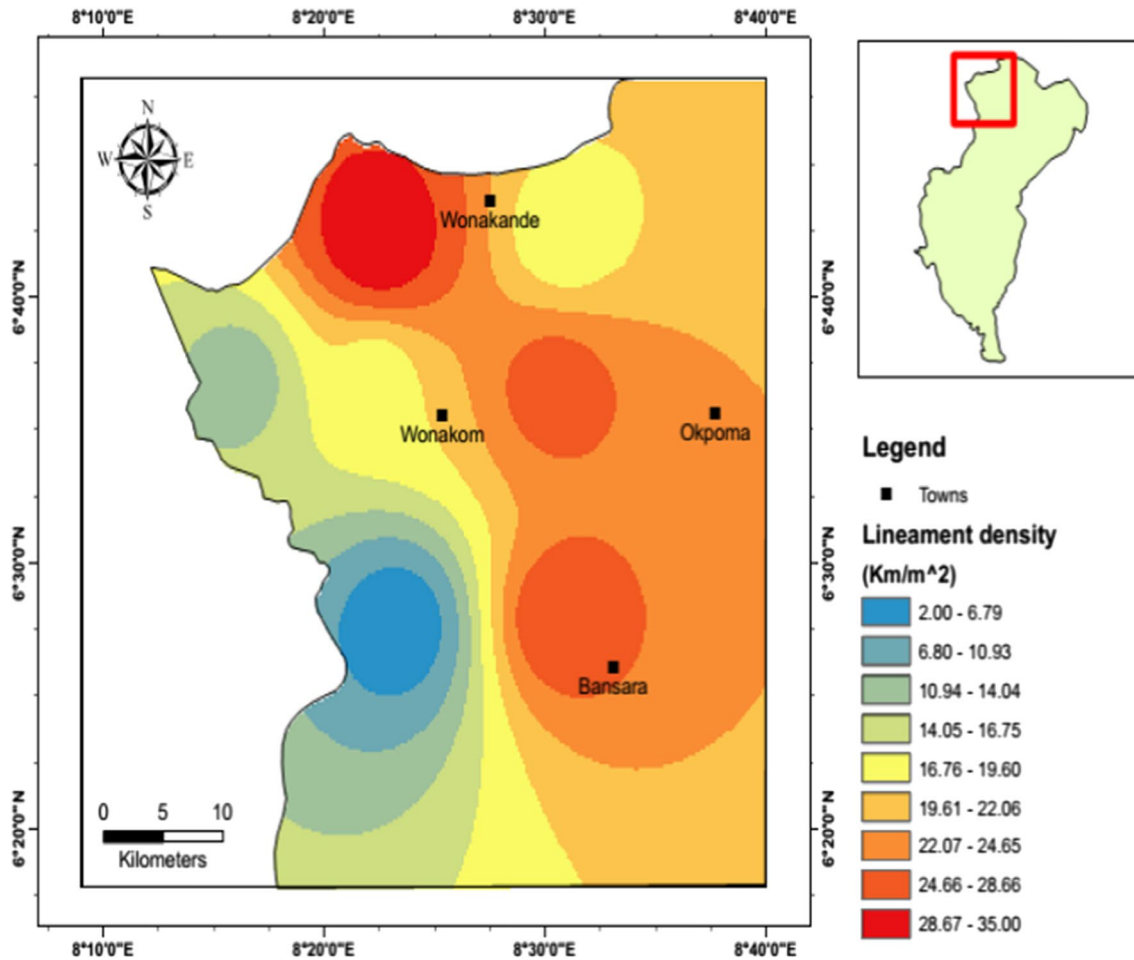
Fig. 5 Lineament length density map of Yala area

measured the potential difference. In the Schlumberger array, the four electrodes were arranged linearly with different inter-electrode spacing, while the potential electrodes remain partially fixed, the current electrodes were expanded symmetrically about the centre of the spread (Dobrin 1976; Telford et al 1978; Parasnis 1986) to a maximum of 500 m in this study. The apparent resistance (R_a) was read from the display of the Terrameter during the survey process. Apparent resistivity was calculated by multiplying the apparent resistance (R_a) by geometric factor (G) given as (Bello et al. 2019; Umar and Igwe 2019):

$$G = \pi \left[(AB/2)^2 - (MN/2)^2/MN \right] \tag{2}$$

The observed field data were then converted to apparent resistivity (ρ_a) using Eq. 3.

$$\rho_a = GR_a = \pi \left(\left[(AB/2)^2 - (MN/2)^2/MN \right] \right) * R_a \tag{3}$$

The calculated ρ_a was plotted against electrode spacing (AB/2) and interpretation done by methods outlined

in Zhody et al. (1974) and Edet and Okereke (1997) on a bi-logarithmic graph paper characterized by a dynamic range for smoothing and correction of outliners, which constituted noise. The smoothened curves were inverted to true resistivity using INTEPEX 1-D (IXID) Version 2.06 least square interactive inversion software program for ID resistivity inversion. The program generates VES curves, together with the geoelectric layer resistivity, thickness and depth (Nwachukwu et al. 2019; Obiora and Ibuot 2020).

Drilling of boreholes was made by standard rotary method to obtain information on lithology, water levels and aquifer parameters. Moreover, to compliment areas without estimates of aquifer parameters from boreholes, surface resistivity data were used to estimate aquifer parameters based on the principles of electric and groundwater flow. These parameters are expressed as:

$$T = Kh \tag{4}$$

Fig. 6 Typical plots of vertical electrical data representing the different curve types in the study area: **a** Q type (UK 2), **b** H type (UK 4), **c** K type (UK 37), **d** HK type (UK 1) and **e** KH type (UK 28)

where T, K and h are aquifer transmissivity, hydraulic conductivity and saturated thickness, respectively. From results of surface resistivity measurements, Dar Zarrouk parameters were computed as (Maillet 1947; Bhattacharya and Patra, 1968; Asfahani 2016):

$$R = h\rho_a \tag{5}$$

$$C = h/\rho a \tag{6}$$

where R and C are aquifer transverse resistance (Ω m^2) and longitudinal conductance (Ω^{-1}), respectively.

A relationship between aquifer transmissivity (T), the transverse resistance (R) and the longitudinal conductance (C) has been established (Niwas and Singhal 1981). Therefore, Eqs. 4, 5 and 6 can be combined to give Eqs. 7 and 8 (Massound et al 2010):

$$T = (K\sigma R) \tag{7}$$

$$T = (K/\sigma)C \tag{8a} \text{ and}$$

$$K = T/h \tag{8b}$$

where σ is water conductivity (Siemens/m or µS/cm). In areas of similar geological and water quality characteristics, the product $K\sigma$ will remain fairly constant (Niwas and Singhal 1981; Mbonu et al. 1991; Onuoha and Mbazi 1988; Tizro et al. 2010). Therefore, if K values are known from pumping test and σ from resistivity measurements, it is possible to calculate transmissivity and its variations over the entire aquifer.

Groundwater sampling, analysis and assessment

Twenty-nine (29) samples of groundwater were collected from existing potable water sources for hydrochemical studies. Fast changing physical parameters (Temp, pH, conductivity, total dissolved solids) were measured in situ using standard field equipment (WTW temperature/conductivity meter LF 90, Oakton TDS/temperature meter (temperature), Hanna HI 9835 conductivity/TDS meter (electrical conductivity, TDS), WTW pH/Eh meter pH90 (pH and Eh) and Hanna HI 8314 pH/Eh meter (pH and Eh). Calibration of these equipment was done using appropriate standard solution provided by the manufacturers. Alkalinity (HCO$_3^-$) of the samples was determined by titration shortly after sampling. Cations were analyzed with flame photometer (Na$^+$,
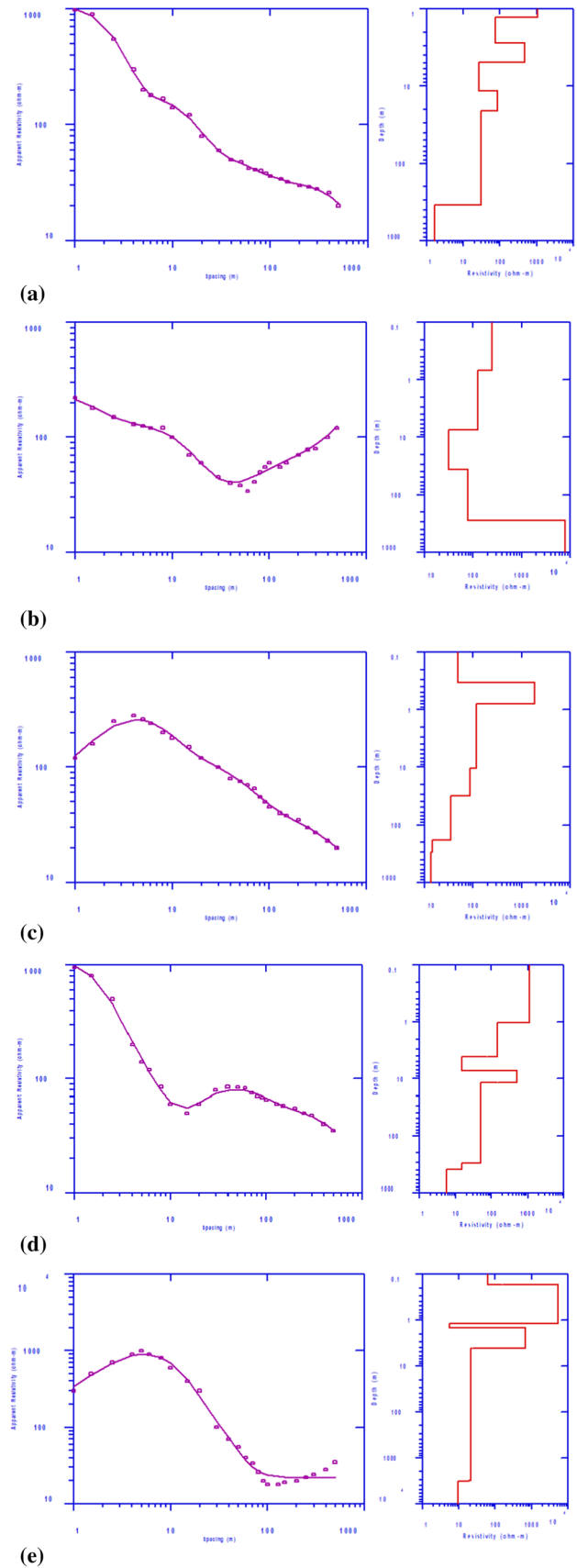

(a)

(b)

(c)

(d)

(e)

Table 1 Summary of results of VES survey showing geoelectric layer resistivities and thicknesses in different groups (Location of VES data shown in Fig. 3)

No	Code	Curve type	Hydrogeo-electrcGroup	Layer resistivity ρ_a (Ω m)					Layer thickness t (m)			
				ρ_1	ρ_2	ρ_3	ρ_4	ρ_5	t_1	t_2	t_3	t_4
1	UK 2	Q	1	1500.0	1000.0	60.0	42.0		0.50	1.00	9.00	
2	UK 31	Q		2500.0	1000.0	25.0	15.0		0.10	2.00	40.00	
3	UK 35	Q		1800.0	2500.0	50.0	55.0	33.00	0.50	1.30	5.00	45.00
4	UK 45	Q		1400.0	1600.0	32.0	40.0	24.00	0.70	2.40	6.00	4.00
5	UK 1	HK	2	1200.0	245.0	28.0	128.0	46.00	0.97	1.90	4.40	21.60
6	UK 24	HK		1145.0	194.0	22.0	174.0	18.00	0.50	2.00	21.00	14.00
7	UK 33	H		3500.0	300.0	42.0	105.0		0.70	5.00	40.00	
8	UK 27	Q	3	750.0	1000.0	30.0	24.0		0.80	3.00	40.00	
9	UK 28	KH		600.0	1500.0	60.0	15.0	30.00	0.50	16.00	12.00	55.00
10	UK 29	Q		1700.0	1500.0	30.0	24.0		0.50	1.50	30.00	
11	UK 4	H	4	180.0	110.0	36.0	44.0		0.70	8.00	28.00	
12	UK 12	HK		200.0	100.0	40.0	60.0	36.00	0.70	2.50	5.00	3.00
13	UK 13	H		180.0	100.0	39.0	45.0		0.60	1.30	8.00	
14	UK 37	K		180.0	150.0	20.0	24.0		4.50	2.00	25.00	
15	UK 48	Q		259.0	140.0	30.0	15.0		1.40	2.00	30.00	
16	UK 3	HK	5	300.0	14.0	30.0	70.0	21.00	0.60	13.00	45.00	40.00
17	UK 25	Q		200.0	38.0	11.0			4.00	25.00		
18	UK 32	Q		134.0	29.0	17.0	39.0		6.50	18.00	94.00	
	Mean		1	1800.0	1525.0	41.8	38.0	28.5	0.5	1.7	15.0	24.5
	Min			1400.0	1000.0	25.0	15.0	24.0	0.1	1.0	5.0	4.0
	Max			2500.0	2500.0	60.0	55.0	33.0	0.7	2.4	40.0	45.0
	Mean		2	1948.3	246.3	30.7	135.7	32.0	0.7	3.0	21.8	17.8
	Min			1145.0	194.0	22.0	105.0	18.0	0.5	1.9	4.4	14.0
	Max			3500.0	300.0	42.0	174.0	46.0	1.0	5.0	40.0	21.6
	Mean		3	683.3	1333.3	40.0	21.0	30.0	0.6	6.8	27.3	55.0
	Min			600.0	1000.0	30.0	15.0	30.0	0.5	1.5	12.0	55.0
	Max			750.0	1500.0	60.0	24.0	30.0	0.8	16.0	40.0	55.0
	Mean		4	199.8	120.0	33.0	37.6	36.0	1.6	3.2	19.2	3.0
	Min			180.0	100.0	20.0	15.0	36.0	0.6	1.3	5.0	3.0
	Max			259.0	150.0	40.0	60.0	36.0	4.5	8.0	30.0	3.0
	Mean		5	211.3	27.0	19.3	54.5	21.0	3.7	18.7	69.5	40.0
	Min			134.0	14.0	11.0	39.0	21.0	0.6	13.0	45.0	40.0
	Max			300.0	38.0	30.0	70.0	21.0	6.5	25.0	94.0	40.0

ρ_a Apparent resistivity (Ω m), t thickness (m)

K^+) and atomic absorption photometer, AAS (Ca^{2+}, Mg^{2+}), while the anions (Cl^-, SO_4^{2-}, NO_3^-) were analyzed with ion chromatography (APHA, 1998). Charge balance error (CBE) was used to determine the level of error in the data. The error ranged between -10 and 10%, indicating an excess amount of cations which is attributed to dilution and to some constituents that precipitated during groundwater movement (Fritz 1994; Grzybowski et al. 2019). Suitability of the samples for drinking and domestic use was based on WHO (2011) guidelines. Irrigation water quality was evaluated by means of hardness, salinity (conductivity) and sodium adsorption ratio (SAR) calculated as follows:

$$SAR = Na^+ / \left(\left[Ca^{2+} + Mg^{2+} \right]/2 \right)^{1/2} \qquad (9)$$

where ion concentrations are expressed in meq/l.

Locations of vertical electrical sounding, static water level, lithologic and water quality data used in the study are presented in Fig. 3 and supplementary material 1.

Fig. 7 Interpretation of resistivity sounding alongside with observed logs at UK 1, UK 4 and UK 33 in the study area
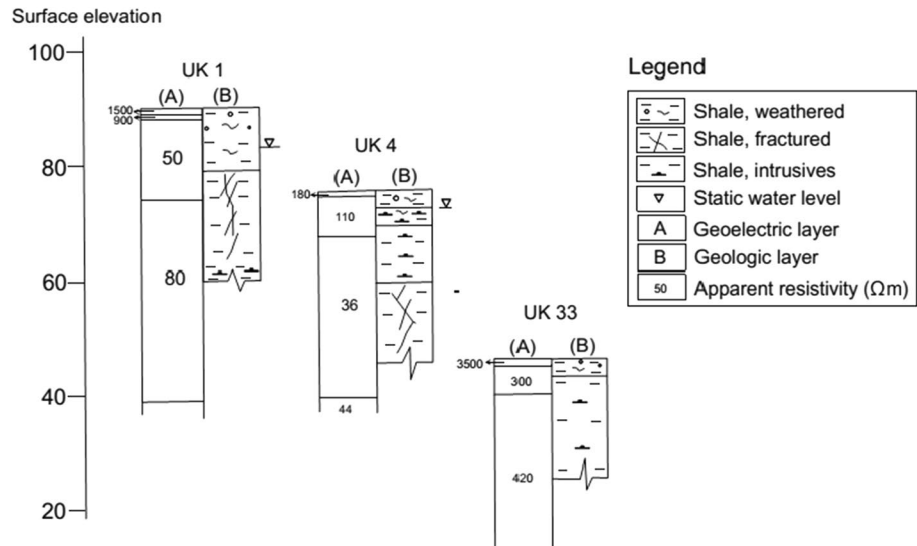
Results

Lineament mapping

Lineament and lineament length density maps of Yala Area are presented as Figs. 4 and 5. The lineaments trend generally in northeast/southwest and northwest/southeast directions with azimuths of 40–50°/220–230° and 140–150°/320–330°. Lineament lengths varied between 0.8 and 13.8 km with an average of 4.7 km and the most frequent lengths being between 2 and 4 km with average of 38.4 km. This range of lineament constituted about 44% of all the mapped lineaments in the area.

The lineaments in form of fractures are linear, crisscrossing and penetrative and are consistent with producing shallow water wells in the area as observed at Bansara (UK 48). Lineament (Fig. 4) and lineament length density (Fig. 5) maps indicate high ($> 22\ \mathrm{m^{-1}}$), low ($< 14\ \mathrm{m^{-1}}$) and moderate (> 14–$< 22\ \mathrm{m^{-1}}$) lineament densities in the north, east and central parts of Yala, suggesting high, low and moderate groundwater potentials. However, aquifer parameters are not available to support this. Studies by Greenbaum (1985, 1989), Tennakon TMTB (1989), Edet (1993a, 1996), Edet et al (1994, 1998), and Edet and Okereke (2005) have reported significant relations between high yielding boreholes and high lineament density. Tectonic activities at various times in the Benue Trough have been linked to the development these of lineaments, followed by intrusion of basaltic rocks in Yala Area (Hossain, 1981; Ofoegbu 1990). McDonald et al. (2001), also noted that these fractures are due to stress unloading, enhanced by dissolution.

Electrical resistivity studies

Eighteen vertical electrical soundings (VESs) were made and examples of curves derived from the data are shown in Fig. 6. The geoelectric sections revealed that the area is characterized by mainly four and five geoelectric layers with the exception of VES location 25, which showed a three layer section of Q type curve ($\rho_1 > \rho_2 > \rho_3$). The four layer geoelectric curves are characterized by Q type curve ($\rho_1 > \rho_2 > \rho_3 > \rho_4$) at UK 2, UK 27, UK 29, UK 31, UK 32 and UK 48, H ($\rho_1 > \rho_2 < \rho_3 < \rho_4$), at UK 4, UK 13 and UK 33, K ($\rho_1 > \rho_2 < \rho_3 < \rho_4$) at UK 37. The five layer curves were characterized by Q type curves ($\rho_1 > \rho_2 > \rho_3 > \rho_4 > \rho_5$) at UK 35 and UK 45, HK ($\rho_1 > \rho_2 < \rho_3 > \rho_4 > \rho_5$) at UK 1, UK 3, UK 12 and UK 24 and KH ($\rho_1 < \rho_2 > \rho_3 > \rho_4 > \rho_5$) at UK 28. The constructed geoelectrical resistivity model show five different subsurface hydrogeoelectric sequence (Table 1 and Figs. 7 and 8).

The first hydrogeoelectric group consist of 4 (UK 2, UK 31) and 5 (UK 35, UK 45) geoelectric layers. VES locations UK 2, UK 31, UK 35 and UK 45 revealed a top layer composed of dry loose reddish yellowish unconsolidated silty, sandy, gravelly highly weathered shale with thickness and resistivity in the range 0.1–0.7 m (mean 0.5 m) and 1400–2500 Ω m (mean 1800), respectively. The top layer is underlained by slightly conductive layer with resistivity and thickness in the range 1000–2500 Ω m (mean 1525 Ω m) and 1.0–2.4 m (mean 1.7 m). The first and the second geoelectric layers does not hold any prospect for groundwater. The second layer is followed by a highly conductive layer with resistivity and thickness in the range 25–60 Ω m (mean 41.8 Ω m) and 5.0–40.0 m (mean 15.0 m). The layer is made up of compact, baked fractured shale. The third layer is underlained by another compact, baked fractured shale having thickness in the range 4.0–45.0 m

Fig. 8 Typical hydrogeoelectric models deciphering the different aquifers in Yala Area based on Table 1
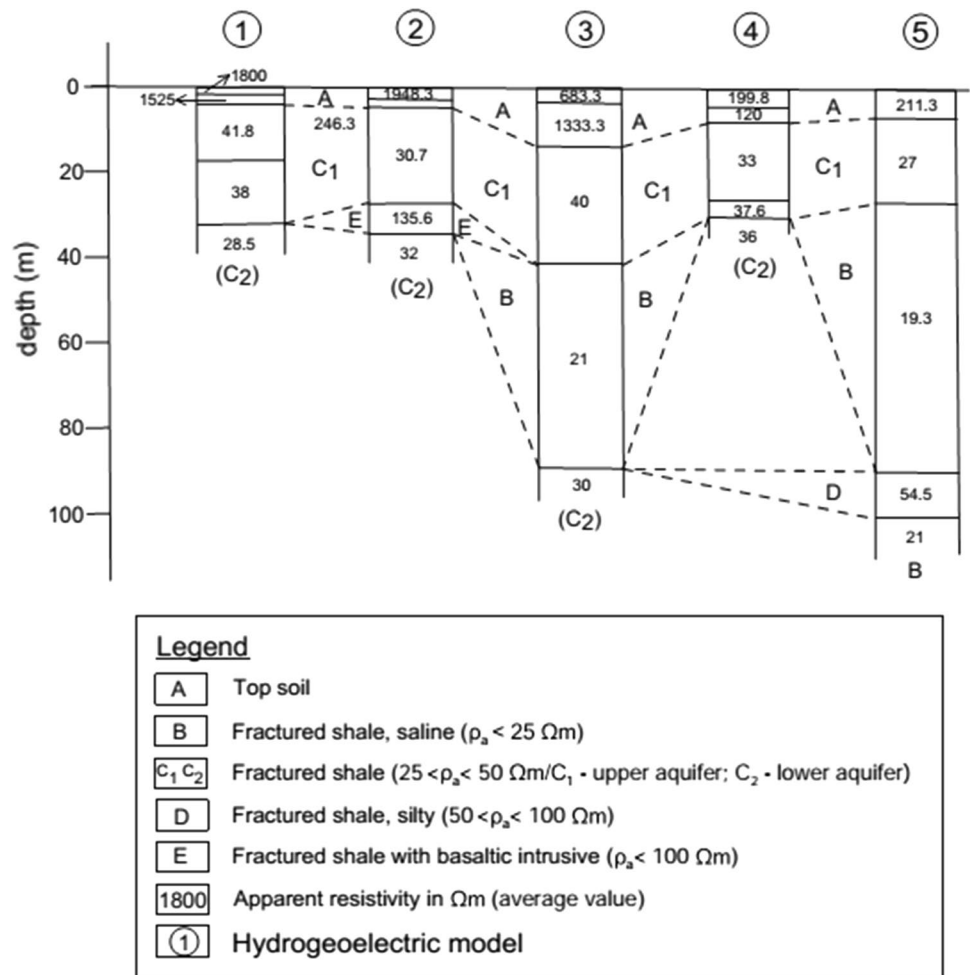
(mean 24.5 m) and resistivity 15–55 Ω m (mean 38 Ω m). The fifth layer with unresolved thickness had resistivity in the range 24.0–33.00 Ω m (mean 28.5 Ω m). The layer is composed of soft fractured shale. In this group, the third and fourth layers constitute the first aquifers in the Yala

Area, while the fifth layer constitute the second aquifer (Fig. 8). Low resistivity (< 25 Ω m) at UK 31 and UK 45 suggest saline shale.

The second hydrogeoelectric group consist of one 4 (UK 3) and two 5 (UK 1, UK 24) geoelectric layers. The first layer is composed of the same materials as in group 1. This layer has thickness in the range 0.5–1.0 m (mean 0.7 m) and resistivity 1145–3500 Ω m (mean 1948.3 Ω m). The top layer is followed by a moderately conductive layer with resistivity in the range 194–300 Ω m (mean 246.3 Ω m) and thickness 1.9–5.0 m (mean 3.0 m). This layer is composed of silty sandy weathered shale. The third layer in this group had resistivity in the range 22–42 Ω m (mean 30.7 Ω m) and thickness 4.4–40.0 (mean 21.8 m) and is composed of compact, baked fractured shale and constitute the first aquifer. Low resistivity at UK 24 (22 Ω m), suggest saline shale. The fourth layer had resistivity in the range 105.0–174.0 (mean 135.7 Ω m) and thickness 14.0–21.6 m (mean 17.8 m). This layer is composed of compact baked weathered shale with basaltic intrusive. This layer constitute a basaltic intrusive, fractured shale aquifer (Fig. 8). The fifth layer interpreted as soft fractured shale with resistivity in the range 18–46 Ω m
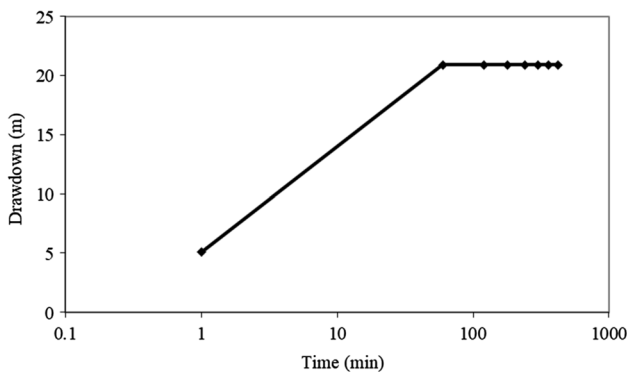

Fig. 9 Drawdown-time plot based on pumping test at Okpoma (UK 45)

Table 2 Estimated transmissivity values obtained from k/σ with C (Location of VES data shown in Fig. 3)

No	Aquifer	Parameter/location	UK 1	UK 2	UK 3	UK 4	UK 12	UK 13	UK 24	UK 27	UK 28	UK 29
1	Upper weathered Shale Aquifer	Average field hydraulic conductivity, K (m/day)	1.15	1.15	1.15	1.15	1.15	1.15	1.15	1.15	0.04	1.15
2		Transmissivity (m²/day)	8.61	8.61	8.61	8.61	8.61	8.61	8.61	8.61	1.97	8.61
3		Aquifer resistivity (Ω m)	28	60	30	36	40	39	22	30	60	30
4		Aquifer thickness (m)	4.4	9	45	28	5	8	21	40	12	30
5		Aquifer longitudinal conductance (Ω^{-1})	0.16	0.15	1.5	0.78	0.13	0.21	0.95	1.33	0.2	1
6		Aquifer transverse resistance (Ω m²)	123.2	540	1350	1008	200	312	462	1200	720	900
7		$\sigma = 1/\rho$	0.036	0.017	0.033	0.028	0.025	0.026	0.045	0.033	0.017	0.033
8		K/σ value	32.2	69	34.5	41.4	46	44.85	25.3	34.5	2.4	34.5
9		$K\sigma$	0.041	0.019	0.038	0.032	0.029	0.029	0.052	0.038	0.001	0.038
10		Transmissivity of aquifer (m²/day)	5.06	10.35	51.75	32.2	5.75	9.2	24.15	46	0.48	34.5
11		Hydraulic conductivity of aquifer K (m/day)	1.15	1.15	1.15	1.15	1.15	1.15	1.15	1.15	0.04	1.15
1	Lower fractured Shale Aquifer	Average field hydraulic conductivity, K (m/day)	1.15				1.15		1.15		0.04	
2		Transmissivity (m²/day)	8.61				8.61		8.61		1.97	
3		Aquifer resistivity (Ω m)	128				60		174		15	
4		Aquifer thickness (m)	21.6				3		14		55	
5		Aquifer longitudinal conductance (Ω^{-1})	0.169				0.05		0.08		3.667	
6		Aquifer transverse resistance (Ω m²)	2765				180		2436		825	
7		$\sigma = 1/\rho$	0.008				0.017		0.006		0.067	
8		K/σ value	147.2				69		200.1		0.6	
9		$K\sigma$	0.009				0.019		0.007		0.003	
10		Transmissivity of aquifer (m²/day)	24.84				3.45		16.1		2.2	
11		Hydraulic conductivity of aquifer K (m/day)	1.15				1.15		1.15		0.04	

No	Aquifer	Parameter/location	UK 31	UK 32	UK 33	UK 35	UK 37	UK 45	UK 48	Min	Mean	Max
1	Upper weathered shale aquifer	Average field hydraulic conductivity, K (m/day)	1.15	1.15	1.15	1.15	1.15	1.49	1.15	0.04	1.1	1.49
2		Transmissivity (m²/day)	8.61	8.61	8.61	8.61	8.61	10.43	8.61	1.97	8.33	10.43
3		Aquifer resistivity (Ω m)	25	17	42	50	20	32	30	17	34.76	60
4		Aquifer thickness (m)	40	94	40	5	25	6	30	4.4	26.02	94
5		Aquifer longitudinal conductance (Ω^{-1})	1.6	5.53	0.95	0.1	1.25	0.19	1	0.1	1	5.53
6		Aquifer transverse resistance (Ω m²)	1000	1598	1680	250	500	192	900	123.2	760.89	1680
7		$\sigma = 1/\rho$	0.04	0.059	0.024	0.02	0.05	0.031	0.033	0.02	0.03	0.06
8		K/σ value	28.75	19.55	48.3	57.5	23	47.68	34.5	2.4	36.7	69
9		$K\sigma$	0.046	0.068	0.027	0.023	0.058	0.047	0.038	0	0.04	0.07
10		Transmissivity of aquifer (m²/day)	46	108.1	46	5.75	28.75	8.94	34.5	0.48	29.26	108.1
11		Hydraulic conductivity of aquifer K (m/day)	1.15	1.15	1.15	1.15	1.15	1.49	1.15	0.04	1.1	1.49

Table 2 (continued)

No	Aquifer	Parameter/location	UK 31	UK 32	UK 33	UK 35	UK 37	UK 45	UK 48	Mean	Min	Max
1	Lower fractured shale aquifer	Average field hydraulic conductivity, K (m/day)				1.15		1.49		1.04	0.04	1.49
2		Transmissivity (m^2/day)				8.613		10.43		7.92	1.97	10.43
3		Aquifer resistivity (Ω m)				55		40		77.43	15	174
4		Aquifer thickness (m)				45		4		26.09	3	55
5		Aquifer longitudinal conductance (Ω^{-1})				0.818		0.1		0.78	0.05	3.67
6		Aquifer transverse resistance (Ω m^2)				2475		160		1662.97	160	2800
7		$\sigma = 1/\rho$				0.018		0.025		0.02	0.01	0.07
8		K/σ value				63.25		59.6		88.61	0.6	200.1
9		$K\sigma$				0.021		0.037		0.02	0	0.04
10		Transmissivity of aquifer (m^2/day)				51.75		5.96		21.47	2.2	51.75
11		Hydraulic conductivity of aquifer K (m/day)				1.15		1.49		1.04	0.04	1.49

ρ_a, electrical resistivity of aquifer (Ω m); t, aquifer thickness (m); C, longitudinal conductance; K, hydraulic conductivity (m/day); σ, electrical conductivity (Siemens/m); T, Transmissivity (m^2/day). K/σ, constant. At the reference borehole (UK 45, Okpoma), the K/σ constant was calculated by using the K obtained from pumping test of the borehole ($K = 1.49$ m/day) and σ obtained from VES data at same station UK 45 ($\sigma = 1/\rho = 1/38$ Ω m = 0.03 Siemens/m). Hence $k/\sigma = 1.49/0.03 = 49.67$. Transmissivity values have been estimated at all sampled sites from the relation $T = (K/\sigma) S = 49.67$ Hydraulic conductivity: Hydraulic conductivity values were obtained at all sample sites from the relation $K = T/t$. Min minimum, Max maximum, SD standard deviation

(mean 32 Ω m) and unresolved depth constitute the second aquifer. Low resistivity at UK 24 (18 Ω m), suggest saline shale aquifer.

Hydrogeoelectric group 3 include 4 (UK 27, UK 28) and 5 (UK 29) layer geoelectric curves. The top layer had resistivity in the range 600–750 Ω m (mean 683.3 Ω m) and thickness 0.5–0.8 m (mean 0.6 m). This layer is interpreted as dry reddish yellowish silty, sandy, highly weathered shale. The top layer is underlained by a resistive layer with resistivity in the range 1000–1500 Ω m (mean 1333.3 Ω m) and thickness 3.8–16.5 m (mean 11.9 m). The layer is interpreted as silty, sandy, gravelly weathered shale. The second layer is underlained by a highly conductive layer with resistivity in the range 30–60 Ω m (mean 40.0 Ω m) and thickness 1.5–16.0 m (mean 6.8 m). This layer is interpreted as compact, baked fractured shale and constitute the first fractured shale aquifer. The fourth layer with resistivity in the range 15–24 Ω m (mean 21.0 Ω m) and thickness in the range 12.0–40.0 m (27.3 m) is interpreted as saline shale aquifer (Fig. 8). The fifth layer with resistivity of 30 Ω m and unresolved thickness at UK 28 is composed of soft fractured shale and constitute the second shale aquifer.

The fourth hydrogeoelectric group includes 4 (UK 4, UK 13, UK 37, UK 48) and 5 (UK 12) geoelectric models. The top layer is interpreted as silty sandy weathered shale with resistivity and thickness in the range 180.0–259.0 Ω m (mean 199.8 Ω m) and 0.6–4.5 m (mean 1.6 m). The top layer is underlain by a slightly conductive layer with resistivity ranging 100.0–150 Ω m (mean 120 Ω m) and thickness 1.3–8.0 m (mean 3.2 m). This layer is interpreted as silty weathered shale. The third layer had resistivity in the range 20.0–40.0 (mean 33.0) and thickness 5.0–30.0 m (mean 19.2 m). This layer is interpreted as compact, baked fractured shale. The fourth layer is another compact, baked fractured shale with thickness of 3.0 m and resistivity in the range 15.0–60.0 Ω m (mean 37.6 Ω m). The third and fourth layers constitute the first shale aquifer with saline shale at UK 37 having resistivity in the range 20.0–24.0 Ω m at depth 6.50 m–α and at UK 48 with resistivity of 15 Ω m and unresolved thickness (Table 1). The fifth layer observed at UK 12 had a resistivity value of 36 Ω m and unresolved thickness was interpreted as soft fractured shale and constitute the second fractured shale aquifer.

Hydrogeoelectric group 5 include 3–(UK 25), 4–(UK 32) and 5–(UK 3) geoelectric layer. The first layer with resistivity in the range 134–300.0 Ω m (mean 211.3 Ω m) and thickness in the range 0.6–6.5 m (mean 3.7 m) is composed of silty sandy weathered shale. The top layer is underlain by a highly conductive layer with resistivity in the range 14.0–38.0 Ω m (mean 27.0 Ω m) and thickness 13.0–25.0 m (mean 18.7 m). This layer is composed of compact, baked fractured shale with saline shale at a depth of 13.6 m and 24.8 m at UK 3 and UK 32 respectively. The third layer

Table 3 Water table (in m below ground surface) fluctuation at Okpoma (UK 45) and Ndok-Ogoja with rainfall data for comparison in 2008

S/N	Location	North	East	Water table			
	characteristics			March	May	October	November
1	Okpoma (UK 45)	6° 35.971	8° 38.486	6.45	6.2	5.65	6.05
2	Ndok-Ogoja	6° 35.979	8° 47.549	4.6	2.75	2.7	3.2
3	Rainfall (mm)	6° 38.752	8° 46.650	0	282.4	398.3	49.4
4	Season			Dry	Dry–wet	Wet	Wet-dry

Table 4 Results of physicochemical parameters for Yala Area

No	Code	pH	EC	TDS	TH	Na^+	K^+	Ca^{2+}	Mg^{2+}	Cl^-	HCO_3^-	SO_4^{2-}	NO_3^-	SAR
1	UK 02	7.6	510	327	253.6	2.1	1.5	75.2	16	0.5	306	8	1	0.1
2	UK 03	8	350	224	171.9	17.0	2.7	44.8	14.6	0.5	200	7	0.5	0.8
3	UK 05	7.7	470	301	225.6	16.3	4.3	44.8	27.7	0.5	288	6	1.5	0.7
4	UK 08	7.7	780	500	335.2	14.1	1.7	53.6	49.08	29	390	7	0	0.5
5	UK 09	8	598	383	177.8	3.9	1.6	48	14.1	12.5	182	10	0.6	0.2
6	UK 10	8.1	820	524	323.3	5.2	1.6	48.8	49.1	16.5	356	5	1.5	0.2
7	UK 11	8.2	800	512	289.4	18.4	1.6	47.2	41.8	1	376	2	2	0.7
8	UK 15	8.4	480	308	205.7	22.7	4.5	40.8	25.3	0.5	282	9	1.5	1.0
9	UK 16	7.8	420	269	194.6	9.4	1.3	55.5	13.61	0.5	238	4	1.2	0.4
10	UK 17	7.7	700	449	213.2	92.9	5.5	32.8	32	0.5	438	18	1	3.9
11	UK 18	8.4	780	500	367.2	9.9	2.7	28.8	72	0.5	440	11	1.1	0.3
12	UK 19	8.5	640	410	131.6	86.9	1.6	26.4	16	0.5	362	5	2	4.6
13	UK 20	7.8	400	256	217.6	8.1	1.5	48	23.8	8	226	6	0.8	0.3
14	UK 21	7.7	450	289	222.0	12.8	1.5	84	2.92	0.5	274	0	1.5	0.5
15	UK 22	8	800	512	131.8	108.1	7	27.2	15.55	35.5	340	13	1.5	5.8
16	UK 23	8.2	888	596	59.9	114.3	2.3	15.2	5.35	1	376	5	1	9.1
17	UK 24	7.4	530	340	189.7	26.4	5.5	55.2	12.6	1	304	6	4	1.2
18	UK 32	8.1	590	378	113.8	104.4	1.9	21.6	14.58	2	334	16	0	6.0
19	UK 38	8.2	20	12.8	8.0	278.7	1.5	2.4	0.49	0.75	604	38	0	60.4
20	UK 39	8	850	545	387.6	1.1	2	30.4	76	0.5	384	10	1	0.0
21	UK 40	8	550	352	171.3	38.4	8.5	21.6	28.6	0.25	288	9	1	1.8
22	UK 41	8.4	550	353	117.9	49.2	1.8	35.2	7.29	2.25	236	9	0.5	2.8
23	UK 43	8.5	1220	782	10.0	261.5	1.6	1.6	1.46	0.5	612	5	1.7	50.6
24	UK 44	7.9	550	353	99.9	42.9	1.6	31.2	5.35	0.75	206	7	0.3	2.6
25	UK 45	8.5	420	269	153.8	19.6	1.3	24.8	22.4	0.5	220	8	0	1.0
26	UK 47	7.65	90	58	42.0	123.4	1.8	14.4	1.5	63.9	73.2	3.8	0.3	11.7
27	UK 48	8.5	850	545	14.0	200.8	1.8	4.8	0.49	0.5	442	19	0.1	32.9
28	UK 49	6.66	140	90	34.0	132.4	1	8	3.4	85.2	36.6	22.2	0.9	13.9
29	UK 50	8.99	1210	776	48.0	201.6	1.2	11.2	4.9	92.3	106.1	3.4	1.1	17.8
WHO (2011)		6.5–8.5	1500	1000	500.0	200.0	12	200	150	250	600	250	50	

EC, Electrical conductivity; TDS, Total dissolved solids; SAR, Sodium adsorption ratio and TH; Total hardness; Units are in mg/L except EC (μS/cm) and pH (no unit)

with thickness in the range 45–94 m at UK 3 and UK 32 and resistivity in the range 11.0–30.0 Ω m (mean 19.3 Ω m) is interpreted as saline shale aquifer. The fourth layer constitute a silty fractured shale aquifer (Fig. 8) had resistivity in the range 39–70 Ω m (mean 54.5 Ω m) and thickness of 40 m at UK 3. The fifth layer with unresolved thickness and resistivity of 21.0 constitute a second saline shale aquifer.

Fig. 10 Hydrogeologic cross section of Yala Area
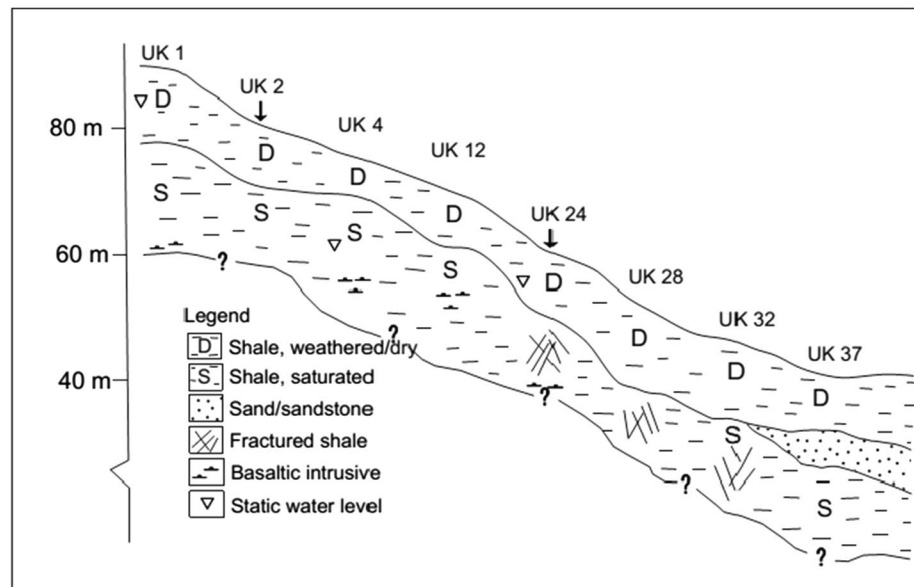
Geological, hydrogeological and hydrochemical studies

Drill logs show that the study area is underlain by a top lateritic dry sandy clay cover ranging in thickness from 8 to 12 m. The top layer is underlain by baked, fractured and compact shale with thickness in the range 12 m and α. In some locations, the shales are intruded by basaltic rocks. The aquifer in Yala is unconfined, with vertical flow of recharge water downwards from upper overlying zone to the lower underlying shale rock which is fractured. A typical geologic and geoelectric section for parts of the study is presented as Fig. 8. Hydraulic parameters are not available for hand-dug wells, HDW (depth < 10 m) and shallow boreholes, SBH (depth > 60 m) as pumping test was not done. Available data for deep boreholes, DBH (depth > 60 m) were based on short duration pumping test conducted by the defunct Federal Ministry of Water Resources (FMWR) on two boreholes at Okpoma, UK 45 and Yahe, UK 46. Figure 9 is a sample drawdown-time time data plot on a semi-log paper for UK 45. Estimates of aquifer parameters from surface resistivity data are presented in Table 2. The results of groundwater table fluctuation monitored at two existing hand dug, one within the study area Okpoma (UK 45) and the other outside Yala Area at Ndok-Ogoja are presented in Table 3. Rainfall data for the same period was also included for comparison.

Table 4 contains results of physical parameters (pH, Electrical conductivity, EC; Total dissolved solids, TDS; Total hardness), cations (Na^+, K^+, Ca^{2+} and Mg^{2+}), anions (HCO_3^-, Cl^-, SO_4^{2-}, and NO_3^-) and irrigation parameter (Sodium adsorption ratio, SAR) of groundwater and WHO (2011) standards for drinking and domestic uses.

Discussion

Hydrogeological conditions and aquifer parameters

In Yala, hand dug well is used to harness water from the upper weathered shale aquifer, as against the use of borehole to exploit the lower fractured shale aquifer (Fig. 10). Groundwater level configuration and flow direction in Yala was possible from water level data from 28 locations. Statistical analysis indicate a minimum value of 1.45 and maximum of 15.00 m (mean 5.90 ± 3.08 m) below the surface. A groundwater table map indicating the flow direction as southwards is presented as Fig. 11. From the groundwater map, absolute groundwater level elevation contours varied from 30 to 60 m. Groundwater level is as high as 65 m at Elahem (UK 1) in the north, while the lowest elevation of 24 m is located in the south at Mfuma (UK 40).

Groundwater fluctuation data (Table 3) show a falling trend during the dry season (March 2008) and a rising trend during wet season (October 2008). In addition, Table (3) shows intermediate values in groundwater levels during the transitional dry–wet season (May 2008) and wet-dry season (November 2008), responding to variation in rainfall and water abstraction. The impact of rainfall during October 2008 with mean rainfall amount of 398.3 mm was to recharge the aquifer. The month of March 2008 was dry with no rainfall (0.0 mm). The rainfall amount increased to 49.4 mm in the month of November 2008 indicating the beginning of the dry season, while May 2008 received 282.4 mm of rainfall signifying the beginning of the rainy season. The low rainfall months of March and November 2008 led to decrease in the amount of stored water in

Fig. 11 Generalized potentiometric map of Yala area based on groundwater levels with respect to the sea level
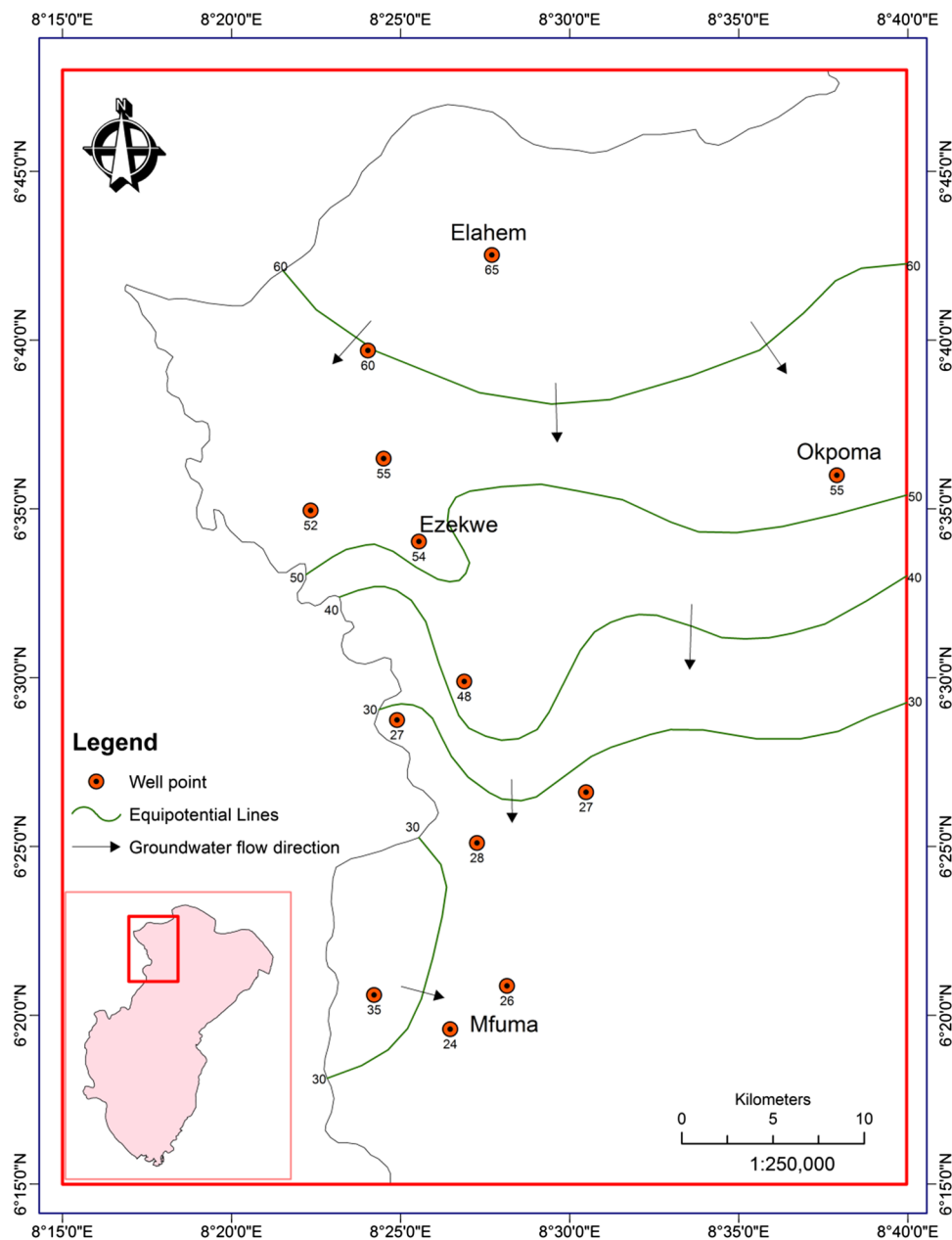
aquifer, especially in the weathered zone due to continued low recharge, high abstraction and evaporation, especially in areas where water level is close to the surface. This thus makes rainfall the major recharge mechanism in Yala Area.

Aquifer transmissivity (T), hydraulic conductivity (K), specific capacity (SC) and well discharge values ranged between 10.43 and 13.44 m^2/day (mean 11.94 m/day) 1.50 and 1.90 m/day (mean of 1.70 m/day) and 4.04 to 5.26 m^3/day/m (mean 4.65m^3/day/m) and 103.70 and 163.20 m^3/day, respectively. Table 2 presents the values of R and C computed from Eqs. 5 and 6 and T from Eqs. 7 and 8. The

parameter Kσ which is constant for the aquifer was estimated for borehole location UK 48. This was combined with transverse resistance values from other locations without pumping test data to determine the transmissivity of the aquifer. The transmissivity values were in the range of 0.48–108.10 m^2/d (mean 29.26 m^2/d) and 2.20–51.75 m^2/d (mean 21.47 m^2/d) for the first and second fractured shale aquifers. The mean hydraulic conductivity were 1.10 and 1.04 m/d, respectively, for upper and lower fractured shale aquifers.
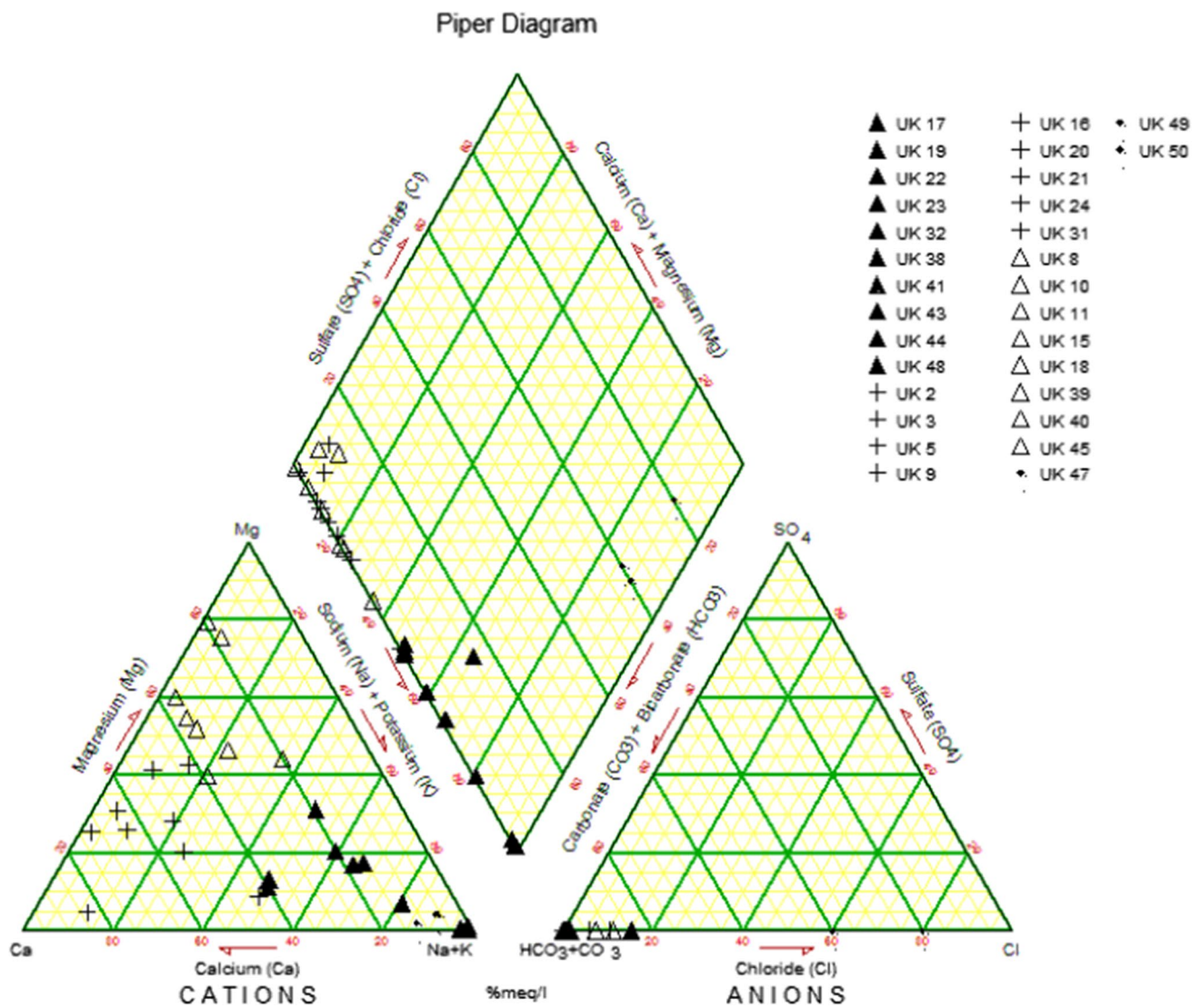
Piper Diagram

Fig. 12 Hydrochemical classification of groundwater using Piper's diagram. Symbols represent different facies. ▲ represent Na^+-HCO_3^-, + represents Ca^{2+}-HCO_3^-, Δ represents Mg^{2+}-HCO_3^- and ● represents Na^+-Cl^-

Physicochemical characteristics, hydrochemical facies and evolution of groundwater

Concentration of hydrogen ions (pH) an indicator of the acidity and alkalinity level of water varied between 6.7 and 9.0 with a mean ± standard deviation (SD) value of 8.0 ± 0.4. Electrical conductivity (EC) varied from 20 to 1220 μS/cm with a mean of 601.9 ± 281.5 μS/cm, while total dissolved solids (TDS) ranged from 12.8 to 782.0 mg/L with a mean of 386.7 ± 181.4 mg/L. The mean values of pH, EC and TDS indicate that the groundwater in Yala Area is of alkaline nature and fresh. The dominant cation in groundwater of Yala Area is sodium (Na^+), while potassium (K^+) constitute the least cation. The concentration of Na^+, K^+,

Ca^{2+} and Mg^{2+} with mean and SD in brackets and units in mg/L varied as follows: 1.1 to 278.1 (69.7 ± 80.1), 1.0 and 8.5 (2.6 ± 1.9 mg/L), 1.6 to 84.0 (33.9 ± 20.6) and 0.5 to 76.0 (20.6 ± 20.2 mg/L), respectively. Samples from three locations (UK 10, UK 18 and UK 39) indicated exceedance of Mg^{2+} over Ca^{2+}, suggesting contributions from dolomites dissolution. In terms of cationic abundance, 31% of Yala groundwater are of $Na^+ > Ca^{2+} > Mg^{2+} > K^+$; 13% $Na^+ > Mg^{2+} > Ca^{2+} > K^+$; 7% each for $Ca^{2+} > Mg^{2+} > Na^+ > K^+$; and $Ca^{2+} > Na^+ > Mg^{2+} > K^+$. Three percent each for $Ca^{2+} > K^+ > Na^+ > Mg^{2+}$; $Mg > Ca^{2+} > K^+ > Na^+$ and $Mg^{2+} > Na^+ > Ca^{2+} > K^+$. This suggest various sources for the cations in groundwater.

Bicarbonate (HCO_3^-) concentration in Yala groundwater varied from 36.6 to 612.0 mg/L (307.6 ± 133.1 mg/L).

Table 5 Chemical composition of different hydrochemical facies[a] (Units in mg/l except EC (µS/cm) and pH (no unit))

Facies	Na⁺–HCO₃⁻			Ca²⁺–HCO₃⁻			Mg²⁺–HCO₃⁻			Na⁺–Cl⁻		
Statistics	Mean	Min	Max	Mean	Min	Max	Mean	Min	Max	Mean	Min	Max
pH	8.20	7.70	8.50	7.75	7.40	8.00	8.16	7.70	8.50	7.77	6.66	8.99
EC	680.80	20.00	1220.00	466.00	350.00	598.00	685.00	420.00	850.00	480.00	90.00	1210.00
TDS	439.08	12.80	782.00	298.63	224.00	383.00	438.75	269.00	545.00	308.00	58.00	776.00
TH	90.01	8.01	213.20	206.58	171.86	253.60	279.19	153.84	387.60	41.33	34.00	48.00
Na⁺	133.97	42.90	278.70	12.00	2.05	26.40	16.17	1.13	38.39	152.47	123.40	201.60
K⁺	2.66	1.50	7.00	2.48	1.25	5.50	2.99	1.30	8.50	1.33	1.00	1.80
Ca²⁺	19.84	1.60	35.20	56.94	44.80	84.00	37.00	21.60	53.60	11.20	8.00	14.40
Mg²⁺	9.86	0.49	32.00	15.67	2.92	27.70	45.54	22.40	76.00	3.27	1.50	4.90
Cl⁻	4.43	0.50	35.50	3.00	0.50	12.50	6.09	0.25	29.00	80.47	63.90	92.30
HCO₃⁻	395.00	206.00	612.00	252.25	182.00	306.00	342.00	220.00	440.00	71.97	36.60	106.10
SO₄²⁻	13.50	5.00	38.00	5.88	0.00	10.00	7.63	2.00	11.00	9.80	3.40	22.20
NO₃⁻	0.81	0.00	2.00	1.39	0.50	4.00	1.02	0.00	2.00	0.77	0.30	1.10
Na⁺/Cl⁻	293.94	4.70	807.27	27.57	0.48	52.54	53.89	0.48	237.02	2.92	2.40	3.37
Na⁺/Na⁺+Cl⁻	0.98	0.82	1.00	0.83	0.33	0.98	0.80	0.33	1.00	0.74	0.71	0.77
Mg²⁺/Ca²⁺+Mg²⁺	0.40	0.15	0.62	0.32	0.05	0.51	0.65	0.51	0.81	0.33	0.15	0.42
HCO₃⁻+SO₄²⁻/Ca²⁺+Mg²⁺	16.14	1.71	66.49	1.03	0.87	1.34	1.07	0.83	1.42	1.65	1.51	1.87

a See Fig. 12 $Mg^{2+}/Ca^{2+} + Mg^{2+}$ = 0.5 dolomite weathering; < 0.5 dolomite-limestone weathering; > 0.5 dolomite dissolution, calcite precipitation or seawater (After Hounslow 1995) $Na^+/Na^+ + Cl^-$ > 1 silicate weathering or ion exchange; 0 halite dissolution (After Hounslow 1995) Na^+/Cl^- > 1 silicate weathering (Meybaek 1987) $HCO_3^- + SO_4^{2-}/Ca^{2+} + Mg^{2+}$ > 1 ion exchange and < 1 reverse ion exchange (Cerling et al. 1989; Fisher and Mullican 1997)
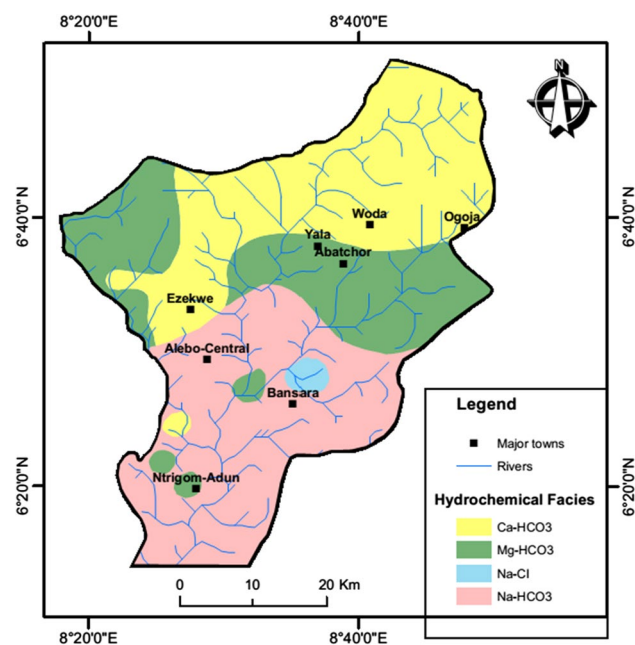
Fig. 13 Map of study area showing spatial distribution of hydrochemical facies

Rock weathering with contribution from CO_2 dissolution constitute the primary source of HCO_3^- (Singh et al. 2013). Chloride concentration ranged from 0.3 to 92.3 mg/L (12.4 ± 25.4 mg/L), constituting 8.1% of the total anion. Chloride in water is assumed to be from atmosphere, dissolution of rock salt or sea water (Singh et al. 2013). Enhanced concentration of Cl^- at UK 8 (29.0 mg/L), UK 15 (35.5 mg/L), UK 47 (63.9 mg/L), UK 49 (85.2 mg/L), and UK 50 (93.3 mg/L) may be attributed to local geochemical process (Edet 1993b). Concentration of sulfate varied between 0.0 and 38.0 mg/L (9.0 ± 7.5 mg/L). Concentration of SO_4^{2-} is usually between 2 and 80 mg/L in natural water and in some cases abnormally high levels (> 1000 mg/L) have been recorded and attributable to industrial discharges and dissolution of gypsum (Chapman 1992; Berner and Berner 1987). This therefore suggest natural sources for sulfate in Yala groundwater. Concentration of nitrate varied between 0.0 and 4.00 mg/L (mean 1.0 ± 0.80 mg/L). Natural levels of NO_3^- seldom exceed 0.1 mg/L (Chapman 1992), but may exceed this value due to application of fertilizers, excreta and waste water disposal. (Apello and Postman 1999; Reddy et al. 2011). With respect to anions, HCO_3^- and Cl^- are the dominant ones followed by SO_4^{2-} and NO_3^- with abundance in the order $HCO_3^- > SO_4^{2-} > NO_3^- > Cl^-$, 43%; $HCO_3^- > SO_4^{2-} > Cl^- > NO_3^-$, 27%; $HCO_3^- > Cl^- > SO_4^{2-} > NO_3^-$, 17%; and $Cl^- > HCO_3^- > SO_4^{2-} > NO_3^-$, 10% and 3%, $HCO_3^- > NO_3^- > Cl^- > SO_4^{2-}$.

Hydrochemical data were plotted on Piper's diagram (Fig. 12). From this, four facies were defined (Table 5): $Na^+ - HCO_3^-$, $Ca^{2+} - HCO_3^-$, $Mg^{2+} - HCO_3^-$ and $Na^+ - Cl^-$. $Na^+ - HCO_3^-$ covers 40% of the hydrochemical data and dominates the discharge area in the south of Yala: $Ca^{2+} - HCO_3^-$ constitutes 30% of all the hydrochemical data and covers the recharge area in the north, while $Mg^{2+} - HCO_3^-$ constitutes 27% of the samples occupied the central parts of the area. Na^+-Cl^- facies constitutes only 3% of the samples and is enclosed within the $Na^+ - HCO_3^-$ facies in the south (Fig. 13). Composition of the different facies (Table 5) shows that the $Ca^{2+} - HCO_3^-$ facies, Ca^{2+} ranged from 44.80 to 84.0 mg/l (mean 56.94 ± 14.76 mg/L), while HCO_3^- varied between 182.0 and 306.0 mg/l (mean 252.25 ± 47.62 mg/L). Mean TDS value for this facies is 298.63 ± 50.71 mg/L, suggesting less mineralization. In this area, the processes contributing ions to this facies is in the descending order dolomite-limestone weathering ($Mg^{2+}/Ca^{2+} + Mg^{2+} < 0.5$, Hounslow, 1995) > silicate weathering ($Na^+/Cl^- > 1$, Meybaek 1987) > ion exchange ($HCO_3^- + SO_4^{2-} > Ca^{2+} + Mg^{2+}$) > reverse ion exchange ($HCO_3^- + SO_4^{2-} < Ca^{2+} + Mg^2$). Discharge area in the south is represented by the Na^+-HCO_3^- facies. Here groundwater movement is sluggish due to drop in elevation and this supported by relatively higher mean TDS of 439.08 ± 199.99 mg/L. The processes involved are of the order weathering of silicate > dolomite-limestone weathering > ion exchange. Central parts of Yala, a mixed recharge-discharge zone is characterized by Mg^{2+}-HCO_3^- with mean TDS of 438.75 ± 110.10 mg/L, also suggest various processes as a dolomite dissolution and/or calcite precipitation ($Mg^{2+}/Ca^{2+} + Mg^{2+} > 0.5$, Hounslow, 1995) > weathering of silicate > exchange of ions. Locations UK 47, UK 49 and UK 50 with $Na^+ - Cl^-$ facies has mean TDS of 308 ± 405.62 mg/L is characterized by saline intrusion.

Ionic ratios presented in Table 6 were applied to unravel the sources of ions in Yala groundwater. Similar technique has been applied by Lee and Song (2007), Singh et al. (2013) and Vinograd and Porowski (2020) to evaluate and understand the chemistry of groundwater in Korea, India and Russia. Three sources have been named as the possible cause ions in groundwater (Berner and Berner 1996). These include (i) atmospheric sources through recharging rain water (ii) weathering of rock and (iii) through human activities. Atmospheric contribution to groundwater chemistry are evaluated using Na^+/Cl^- and K^+/Cl^- ratios (Singh et al. 2013). Mean ratios of Na^+/Cl^- (124.13 ± 206.56) and K^+/Cl^- (3.59 ± 5.86) in Yala groundwater indicates higher values of Na^+ and K^+ compared to marine aerosols with values of 0.85 and 0.0176 (Zhang et al. 1995) for Na^+/Cl^- and K^+/Cl^- respectively. High concentration of Na and K^+ to total cations suggest weathering of silicate minerals

Table 6 Ionic ratios

S/N	Code	Na^+/Cl^-	K^+/Cl^-	$HCO_3^-/Cl^-+SO_4^{2-}$	$Ca^{2+}+Mg^{2+}/HCO_3^-+SO_4^{2-}$	$Ca^{2+}+Mg^{2+}/HCO_3^-$	$Ca^{2+}+Mg^{2+}/TC$	Na^++K^+/TC	Na^++K^+/Cl^-	Ca^{2+}/Na^+	Mg^{2+}/Na^+	HCO_3^-/Na^+
1	UK 2	6.33	2.72	27.75	0.98	1.02	0.98	0.02	9.05	42.19	14.96	56.28
2	UK 3	52.54	4.90	20.50	1.01	1.05	0.81	0.19	57.44	3.03	1.64	4.43
3	UK 5	50.32	7.81	33.95	0.94	0.96	0.85	0.15	58.13	3.16	3.26	6.66
4	UK 8	0.75	0.05	6.64	1.04	1.06	0.91	0.09	0.80	4.37	6.67	10.43
5	UK 9	0.48	0.12	5.32	1.12	1.20	0.94	0.06	0.60	14.12	6.91	17.55
6	UK 10	0.48	0.09	10.26	1.10	1.12	0.96	0.04	0.57	10.90	18.27	26.06
7	UK 11	28.40	1.45	88.26	0.94	0.95	0.87	0.13	29.85	2.95	4.35	7.70
8	UK 15	70.07	8.17	22.93	0.86	0.90	0.79	0.21	78.25	2.07	2.14	4.68
9	UK 16	29.11	2.27	40.05	0.98	1.00	0.90	0.10	31.38	6.77	2.77	9.52
10	UK 17	286.78	9.99	18.45	0.57	0.60	0.51	0.49	296.77	0.41	0.66	1.78
11	UK 18	30.56	4.90	29.65	1.00	1.03	0.94	0.06	35.46	3.35	13.94	16.76
12	UK 19	268.26	2.91	50.18	0.44	0.45	0.41	0.59	271.16	0.35	0.35	1.57
13	UK 20	1.55	0.17	10.57	1.14	1.18	0.92	0.08	1.72	6.86	5.67	10.59
14	UK 21	39.51	2.76	318.92	0.99	0.99	0.88	0.12	42.27	7.55	0.44	8.07
15	UK 22	4.70	0.18	4.39	0.45	0.48	0.35	0.65	4.88	0.29	0.28	1.19
16	UK 23	176.42	2.09	46.58	0.19	0.20	0.19	0.81	178.51	0.15	0.09	1.24
17	UK 24	40.75	4.99	32.54	0.75	0.76	0.75	0.25	45.74	2.40	0.91	4.34
19	UK 32	80.59	0.86	14.05	0.40	0.42	0.33	0.67	81.45	0.24	0.27	1.21
20	UK 38	573.56	1.82	12.18	0.02	0.02	0.01	0.99	575.37	0.01	0.00	0.82
21	UK 39	3.49	3.63	28.30	1.21	1.25	0.99	0.01	7.12	30.94	128.91	128.13
22	UK 40	237.02	30.87	24.27	0.71	0.73	0.65	0.35	267.89	0.65	1.43	2.83
23	UK 41	33.76	0.73	15.42	0.58	0.61	0.52	0.48	34.49	0.82	0.28	1.81
24	UK 43	807.27	2.91	84.84	0.02	0.02	0.02	0.98	810.18	0.01	0.01	0.88
25	UK 44	88.29	1.94	20.23	0.57	0.59	0.51	0.49	90.22	0.84	0.24	1.81
26	UK 45	60.35	2.36	19.95	0.82	0.86	0.78	0.22	62.71	1.46	2.20	4.24
27	UK 47	2.98	0.03	0.64	0.66	0.70	0.14	0.86	3.01	0.13	0.02	0.22
28	UK 48	619.83	3.27	17.68	0.04	0.04	0.03	0.97	623.10	0.03	0.00	0.83
29	UK 49	2.40	0.01	0.21	0.64	1.14	0.11	0.89	2.41	0.07	0.05	0.10
30	UK 50	3.37	0.01	0.65	0.53	0.56	0.10	0.90	3.38	0.06	0.05	0.20
	Min	0.48	0.01	0.21	0.02	0.02	0.01	0.01	0.57	0.01	0.00	0.10
	Max	807.27	30.87	318.92	1.21	1.25	0.99	0.99	810.18	42.19	128.91	128.13
	Mean	124.13	3.59	34.67	0.71	0.75	0.59	0.41	127.72	5.04	7.47	11.45
	SD	206.56	5.86	58.76	0.35	0.37	0.35	0.35	207.69	9.53	23.85	25.10

TC, Total cations

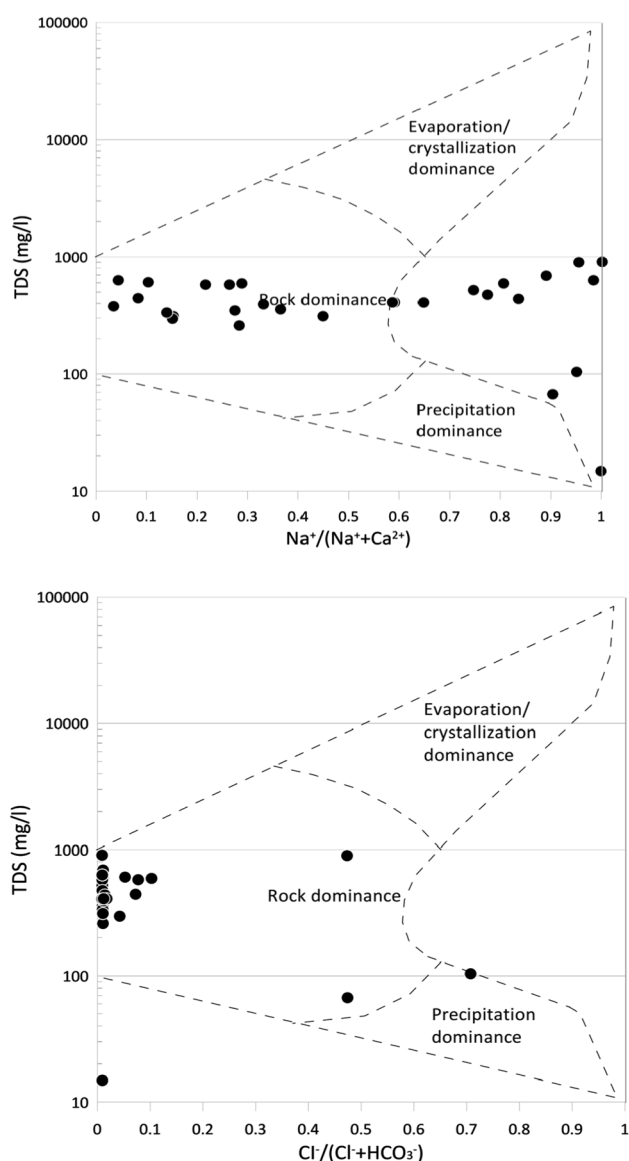**Fig. 14** Mechanisim controlling groundwater chemistry by means of Gibbs (1970) plot in Yala Area. Note Precipitation (TDS < 10 mg/l), Weathering process (10 < TDS < 1000 mg/l) and Evaporation (TDS > 1000 mg/l)

(Al-Mikhlafi et al. 2003). High HCO_3^- concentration and high $HCO_3^-/Cl^- + SO_4^{2-}$ ratio value (mean 34.67 ± 58.76) also suggest weathering as a source of ions (Hounslow 1995; Rose 2002). Weathering as the source of ions in Yala groundwater was supported by the use of Gibbs diagram (Fig. 14). Figure (14) shows that 90% groundwater samples fall within the rock weathering field and 10% of samples lie under precipitation field. Several ionic ratios were applied to decipher the type of weathering responsible for contributing ion to the groundwater. The ratio of $Ca^{2+} + Mg^{2+}/HCO_3 + SO_4^{2-}$ was applied. The value of $Ca^{2+} + Mg^{2+}/HCO_3 + SO_4^{2-}$ varies between 0.02 and 1.21

(mean 0.71 ± 0.35), with 77% of the groundwater samples having values < 1. This suggest contributions from non-carbonate source, while 23% with values > 1, indicate contributions from carbonate minerals. Carbonate weathering demands that the ratio $Ca^{2+} + Mg^{2+}/HCO_3 = 1$. However, $Ca^{2+} + Mg^{2+}/HCO_3$ ratio for Yala groundwater varies between 0.02 and 1.25 (0.75 ± 0.37) with 67% of the samples having values < 1, while 33% had values > 1. Values > 1, suggest carbonate weathering. The ratio of $Ca^{2+} + Mg^{2+}$/total cations (TC) varies between 0.01 and 0.99 (mean 0.59 ± 0.35), reflecting increasing contributions of silicate weathering through Na^+ and K^+. The high mean concentrations Na^+ (mean 69.7 ± 80.1 mg/L) and K^+ (2.6 ± 1.9 mg/L) are higher than the concentration of Cl^- (12.4 ± 25.4 mg/L) and values of $Na^+ + K^+/Cl^-$ in the range 0.57–810.18 (mean 127.72 ± 207.69) suggesting silicate weathering.

To further elaborate on the importance of silicate and carbonate weathering as source of ions in groundwater of Yala, the molar ratio of Ca^{2+}/Na^+, Mg^{2+}/Na^+ and HCO_3^-/Na^+ were applied. These ratios have been used by (Stallard and Edmond, 1983; Meybeck, 1987; Negrel et al. 1993; Gaillardet et al. 1999) to determine the source of ions in water. The values of these ratios for carbonate weathering dominance are 50, 10 and 120 respectively and for silicate weathering 0.35 ± 0.15, 0.24 ± 0.12 and 2.00 ± 1.00, respectively. The mean values for Yala groundwater were 5.04 ± 9.53, 7.47 ± 23.85 and 11.45 ± 25.10, respectively. These values suggest weathering of silicate minerals as the main contributor of ions and carbonate weathering as minor source.

Ion and reverse ion exchange processes are other sources of ions in water. According to Cerling et al. (1989) and Fisher and Mullican (1997) if the ratio $Ca^{2+} + Mg^{2+} < HCO_3 + SO_4^{2-}$, ion exchange dominates, while reverse ion exchange dominates if $Ca^{2+} + Mg^{2+} > HCO_3 + SO_4^{2-}$. In Yala groundwater, 73% of the groundwater show $Ca^{2+} + Mg^{2+} < HCO_3 + SO_4^{2-}$, suggesting ion exchange process indicating Ca^{2+} and Mg^{2+} exchanged for Na^+, while the remaining 27% show $Ca^{2+}Mg^{2+} > HCO_3 + SO_4^{2-}$, suggesting reverse ion exchange and that Na^+ exchanged for Ca^{2+} and Mg^{2+}.

Drinking and irrigation application

Indicators of drinking water quality (TDS, pH, TH, Na^+, K^+, Ca^{2+}, Mg^{2+}, HCO_3^-, SO_4^{2-}, NO_3^-) in most samples are below the admissible limits (MAL) prescribed for drinking water (Table 4). However, 14% of sodium was higher than MAL. Total hardness of Yala groundwater based on the scheme of Sawyer and McCarthy (1967) show that 24 and 14% of the samples fall under soft and

Table 7 Classification of groundwater in Yala Area for irrigation use

Parameters	Class range	Code	Classification	No	%
Total hardness (TH), mg/l	<75		Soft	7	24
(Sawyer & McCarthy 1967)	75–150		Moderately hard	4	14
	150–300		Hard	14	48
	>300		Very hard	4	14
Salinity hazard (Electrical conductivity, EC), μS/cm	<250	C_1	Low salinity (excellent quality)	2	7
(Ragunath 1987)	250–750	C_2	Medium salinity (good quality)	17	59
	750–2250	C_3	High salinity (permissible quality)	10	34
	>2250	C_4	Very high salinity (doubtful quality)		
Sodium adsorption ratio (SAR)	<10	S_1	Excellent	23	80
(Richards 1954)	10–18	S_2	Good	3	10
	18–26	S_3	Doubtful	0	0
	>26	S_4	Unsuitable	3	10
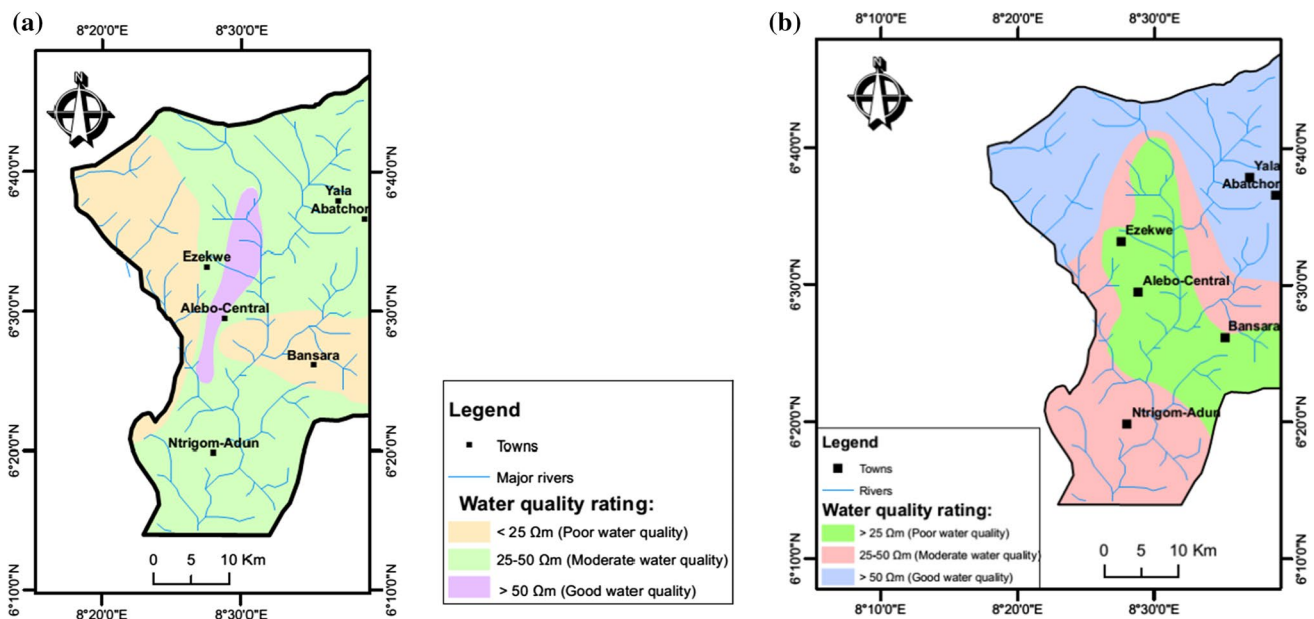
Fig. 15 a Resistivity contour at mean depth < 10 m First aquifer (geoelectric layer 3) showing spatial distribution of different groundwater quality. The aquifer sustain hand dug wells at depth < 10 m **b** Resistivity contour at mean depth > 10 m Second aquifer (geoelectric layer 4) showing spatial distribution of different groundwater quality. The aquifer sustain boreholes at depth > 10 m

moderately hard class, while 48 and 14% fall in the class of hard and very hard (Table 7).

Salinity hazard was used to assess the quality of groundwater for irrigation use (Ravikumar et al 2011). Based on this, 7 and 59% of the groundwater samples from Yala Area are of excellent (C_1) and good (C_2) qualities, while 34% is of permissible quality water (C_3). Also, evaluation using SAR (Richard 1955; Wilcox 1955) indicates that the groundwater samples are of excellent (80%) through good (10%) to poor (10%) water quality (Tables 3 and 7).

Extent of saline water mixing from geophysical and hydrochemical data and guide to groundwater management

Electrical conductivity measurements (350–590 μS/cm) of groundwater samples from nearby wells and boreholes (UK 3, UK 24 and UK 32) is fairly uniform. Thus, variations in resistivity of formation can be assumed as due to variation in lithology (Choudhury et al. 2001). However, groundwater from two locations, UK 43 and UK 50 show relatively
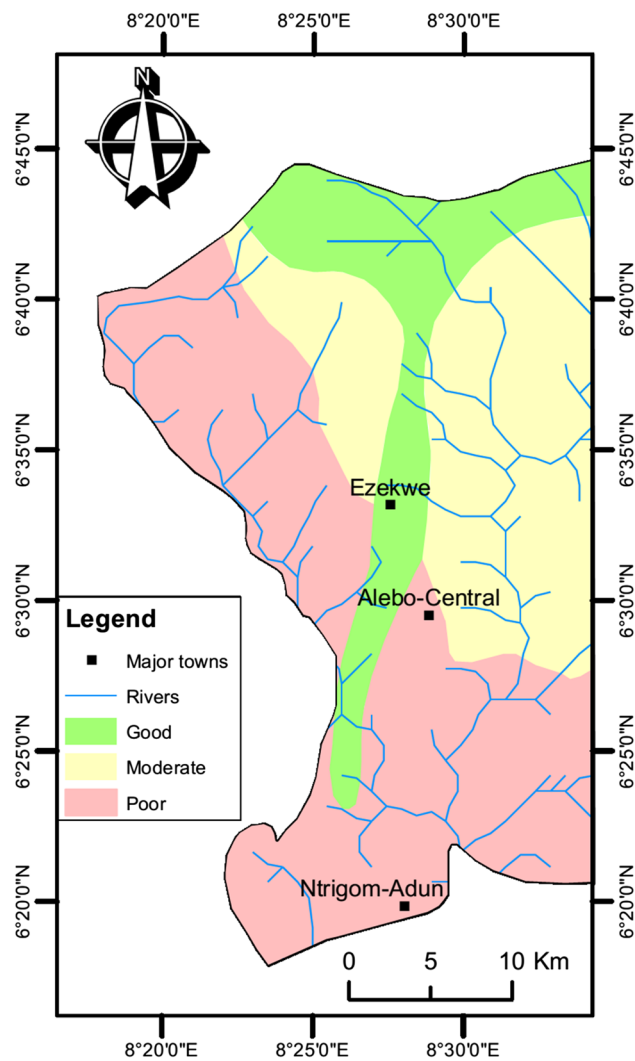
Fig. 16 Groundwater potential map of study area

high electrical conductivity of 1210–1220 µS/cm due to saline water contamination. Choudhury et al. (2001) also showed that resistivity values < 4 Ω m to represent brackish/ saline water zone; 4–7 Ω m, saturated clayey silt; 7–18 Ω m saturated silty, clayey sand and > 18 Ω m saturated sand. Hence, zones characterized by values of formation resistivity as low as 4 Ω m or less represent brackish/saline water saturated formations, while zones with resistivity values > 18 Ω m represent aquifers with freshwater. Edet and Okereke (2001) showed that saltwater contaminated aquifer in southern Nigeria is characterized by low resistivity (< 25 Ω m), while freshwater aquifer is characterized by high resistivity (< 25 Ω m). Antony et al. (2013) also showed resistivity values in the ranges 25–200 Ω m, 7–25 Ω m and 1–7 Ω m to represent freshwater, brackish water and saline water, respectively. In addition, Gabr et al. (2017) gave resistivity values in the range 21–143 Ω m to represent freshwater-saturated clayey sand deposits and favorable for groundwater

accumulation, while values of resistivity in the range 1.7–6.4 Ω m represented saline water-saturated clayey sand deposits as not favorable for potable groundwater accumulation. In a recent study in Abakpa-Ogoja near Yala, Akiang et al. (2020), revealed that saline and brackish water aquifers have resistivity < 12.4 Ω m and > 12.5 Ω m for freshwater aquifers.

In Yala Area, resistivity values in the range 4.8–25 Ω m were attributed to aquifers intruded by saline water. The data are utilized to produce maps at depths < 10 m and > 10 m, which are expected to sustain wells and boreholes and are presented as Fig. 15. The map brings out the horizontal disposition of fresh and saline groundwater. Also, it was essential to determine the minimum value of aquifer resistivity that groundwater cannot be used for drinking and irrigation. Hence, groundwater with TDS > 500 mg/L is considered of poor quality and the mean TDS of Yala groundwater is 386.7 mg/L. However, the higher the TDS, the lower the aquifer resistivity. Therefore, in Yala area characterized by fractured shale containing high TDS groundwater should give rise to low resistivity (< 25 Ω m), which is unsuitable for human use. Relatively high TDS of 500–782 mg/l have been measured from some locations (UK 8, 10, 11, 18, 22, 23, 39, 43, 48 and 50). However, no VES locations are near these water points, except UK 48. Hence, aquifers in Yala with good quality water for human use should be < 25 Ω m. Figure 15a shows a contour map of interpreted geoelectric layer 3 (upper aquifer). Keeping in mind the index resistivity of 25 Ω m, it is interpreted that the southeastern and western parts is occupied by shallow saline groundwater and hence cannot be harnessed. Figure 15b shows resistivity contour map for layer 4 (lower aquifer). The central area covering about 31% is occupied by low resistivity (< 25 Ω m) due to presence of saline groundwater. Geoelectric layers 1 (75–2250 Ω m and depth 0.6–5.4 m) and 2 (8.5–1800 Ω m and thickness 1.0–40.0 m) does not contain appreciable saline water relative to layers 3 and 4. Layer 2 may constitute localized, but not extensive potential freshwater zones at UK 3, 12, 25, 31 and 32. On the basis of this, prospective zones for groundwater with minimum risk for saline groundwater are areas marked as > 25 Ω m values in Fig. 15. Abdul Nassir et al. (2004) and Ukpai and Okogbue (2017) applied similar method in salinized shaly terrain to decipher saline groundwater zones.

High lineaments characterizes the northern parts of Yala with lineament length density (LD) > 30 km^{-1}, while the southwest is characterized by low lineaments, with LD < 10. Moderate lineaments (LD 10–30 km^{-1}) characterizes the central parts of the area (Fig. 4). High borehole yields is expected in the north since borehole yield increases with increase in LD (Edet 1993a). Two aquifers have been delineated for drilling of productive boreholes. The first aquifer (geoelectric layer 3) show that good water quality can be

obtained in central Yala (mean resistivity > 50 Ω m), while the western and southeastern contain water of poor quality (mean resistivity < 25 Ω m). In the north and northeastern, moderate groundwater quality with mean resistivity 25–50 Ω m can be harnessed in the north/northeast. The second aquifer (geoelectric layer 4) contain water of good quality in north and southwestern parts and moderate quality in northwest and northeast. Poor groundwater quality is concentrated in the central parts of Yala (Fig. 15. A groundwater potential map (Fig. 16) on the basis of overlaying lineament density, vertical electrical sounding and hydrochemical data indicate that 25% of the area in the north and central is expected to have good groundwater potential; 36% covering east and western part of the area moderate groundwater potential, while 39% covering west of the good potential area, south of moderate groundwater potential and enclosing south of good groundwater quality as poor groundwater potential.

Conclusions

This study has demonstrated the utilization of geological, geophysical and hydrogeological investigations for delineating potential groundwater areas in a fractured shale rock intruded by saline water. Based on the analysis and evaluation of results, it was possible to delineate four aquifers: an upper weathered, fractured shale aquifer and a lower fractured shale aquifer; fractured saline shale aquifer; fractured shale silty aquifer and basaltic intrusive fractured shale aquifer. The resistivities and thicknesses of the upper fractured shale aquifer were of the range 4.8–180 Ω m and 2.3–209.5 m. The lower fractured shale aquifer with unresolved depth has resistivity values in the range 3.0–220 Ω m. The low resistivity values (< 25 Ω m) were due to isolated saline water intrusion. The potentials of groundwater in the area is limited to the central parts of the upper and north and southwestern parts in the lower aquifer. Majority of groundwater are within the required standard for drinking and domestic use, while for irrigation, the quality varied from suitable to unsuitable. $Na^+ - HCO_3^-$ constitute the main facies water type. Weathering of various types and ion exchange processes are the major sources of ions in water. A groundwater potential map for Yala Area an outcome of this work, delineates good, moderate and poor groundwater potential areas. This map is expected to guide the sustainable development and management of groundwater in Yala and similar areas, especially within the Benue Trough with similar saline water problem in fractured shale.

Supplementary Information The online version contains supplementary material available at https://doi.org/10.1007/s13201-022-01715-2.

Declarations

Conflict of interest The authors hereby declare that they have no conflict of interest.

Data and material All data are provided in the manuscript.

Code availability Not applicable.

References

Abdul Nassir S, Loke M, Nawawi M (2004) Salt-water intrusion mapping by geoelectrical imaging surveys. Geohys Prospect 48:647–661

Agha SO (2015) Groundwater studies in Abakaliki using electrical resistivity method IOSR. J Appl Phys 7(6):5–10

Aghomelu OP, Ezeh HN, Obasi AI (2013) Groundwater exploitation in Abakiliki metropolis (southeastern Nigeria): Issues and challenges. Afr J Environ Sci Technol 7(11):1018–1027

Akiang FB, George AM, Ibeneme SI, Agoha CC (2020) Application of electrical resistivity method in delineating brine contaminated aquifer in Abakpa area, Lower Benue Trough, Nigeria. Int J Innov Sci Res Technol 5(4):247–258

Al-Mikhlafi AS, Das BK, Kaur P (2003) water chemistry of Mansar Lake (India): an indication of source area weathering and seasonal variability. Environ Geol 44:645–653. https://doi.org/10.1007/s00254-003-0798-x

Antony RA, Ramanujam N, Sudarsan R (2013) Delineation of saltwater freshwater interphase in beach groundwater using 2D ERI technique in the northern sector of the Gulf of Mannar coast. Tamilnadu Water J 5:1–11

APHA (1998) Standard methods for the examination of water and waste water, 19th edn. American Public Health Association, Washington DC

Appelo CAJ, Postma D (1999) Geochemistry, groundwater and pollution. Geochemistry, groundwater and pollution. AA Balkema, Rotterdam, the Netherlands, AA Balkema Rotterdam Netherlands

Asfahani J (2016) Hydraulic parameters estimation by using an approach based on vertical electrical sounding (VES) in the semi-arid Khanasser valley region, Syria. J African Earth Sci 117:196–206

Balia R, Ardau F, Barrocu G, Gavaudo E, Ranieri G (2009) Assessment of the Capaterra Coastal plain (southern Sardinia, Italy) by means of hydrogeological and geophysical studies. Hydrogeol J 17:981–997

Bello HI, Alhassan UD, Salako KA, Rafiu AA, Adetona AA, Shehu J (2019) Geoelectrical investigation of groundwater potential at Nigerian Union of Teachers estate, Paggo, Minna Nigeria. Appl Water Sci 9:52. https://doi.org/10.1007/s13201-019-0922-2

Benkhhelil J (1989) The origin and evolution of the Cretaceous Benue Trough. J African Earth Sci 8:251–282

Berner EK, Berner RA (1987) The global water cycle: geochemistry and environment. Prentice-Hall, Englewood Cliffs

Bhattacharya PK, Patra HP (1968) Direct current geoelectric sounding. Elsevier, Amsterdam pp 4–7

Cerling TE, Pedrson BL, Damm KLV (1989) Sodium-calcium ion exchange in weathering of shales. Implic Global Weather Budg Geol 17:552–554

Chapman D (1992) Water quality assessments. Chapman & Hall, London, p 585p

Choudhury K, Saha DK, Chakraborty P (2001) Geophysical study for saline water intrusion in a coastal alluvial terrain. J Appl Geophys 46:189–200

CRBDA Cross River Basin Development Authority (1982) Inventory of natural site conditions-soil, slope, hydrology, land use and vegetation throughout the area of operation of the authority. Progress Report No 4, 145pp

Dobrin MB (1976) Introduction to geophysical prospecting, 3rd edn. McGraw-Hill Book Company, New York

Edet AE (1993b) Groundwater quality assessment in parts of eastern Niger delta, Nigeria. Environ Geol 22:41–46

Edet AE (1996) Evaluation of boreholes sites based on airphoto derived parameters. Bull Int Assoc Eng Geol-Bull De L'assoc Int De Géol De L'ingénieur 54(1):71–76

Edet AE, Okereke CS (1997) Assessment of hydrogeological conditions in basement aquifers of Precambrian Oban massif, southeastern Nigeria. J Appl Geophys 36:195–204

Edet AE, Okereke CS (2001) A regional study of saltwater intrusion in southeastern Nigeria based on analysis of geoelectrical and hydrochemical data. Environ Geol 40(10):1278–1289

Edet AE, Okereke CS (2005) Hydrogeological and hydrochemical character of the regolith aquifer, northern Obudu Plateau, southern Nigeria. Hydrogeol J 13(2):391–415

Edet AE, Teme SC, Okereke CS, Esu EO (1994) Lineament analysis for groundwater exploration in Precambrian Obudu and Oban massif southeastern Nigeria. J Min Geol 30(1):87–95

Edet AE, Okereke CS, Teme SC, Esu EO (1998) Application of remote sensing data to groundwater exploration: A case study of Cross River State, southeastern Nigeria. Hydrogeol J 6:394–404

Edet AE (1993a) Hydrogeology of parts of Cross River State, Nigeria: Evidence from aero-geological and surface resistivity studies, Unpublished Ph. D Thesis of the Department of Geology, University of Calabar, pp 350

Eke KT, Igboekwe MU (2011) Geoelectric investigation of groundwater in some villages in Ohafia Locality, Abia State, Nigeria. British J Appl Sci Technol 1(4):190–203

Ekwere SJ, Ukpong EE (1994) Geochemistry of saline groundwater in Ogoja, Cross River State of Nigeria. Jour Min Geol 30(1):11–15

Fisher RS, Mulican WF (1997) Hydrochemical evolution of sodium-sulphate and sodium-chloride groundwater beneath the Northern Chihuahua desert, Trans-Pecos Texas, USA. Hydrogeol J 5(2):4–16

Fritz S (1994) A survey of charge-balance errors on published analyses of potable groundwater and surface waters. Groundwater 32(4):539–546. https://doi.org/10.1111/j.1745-6584.1994.tb00888.x

Gabr SS, Morsy EA, El Bastawesy MA, Habeebullah TM, Shaaban FF (2017) exploration of potential groundwater resources at Thuwal area, north of Jeddah, Saudi Arabia, using remote sensing data analysis and geophysical survey. Arab J Geosci 10:509. https://doi.org/10.1007/s12517-017-3295-3

Gaillardet J, Dupre B, Louvat P, Allegre JC (1999) Global silicate weathering and CO_2 consumption rates deduced from chemistry of large rivers. Chem Geol 159:3–30

Gibbs RJ (1970) Mechanisms controlling world water chemistry. Science 170:1088–1090

Greenbaum D (1985) Review of remote sensing applications to groundwater exploration in basement and regolith, Br Geol Surv Report OD 85/8, 36 pp

Greenbaum D (1989) Hydrogeological applications of remote sensing in areas of crystalline basement, In: Proceedings groundwater exploration and development in crystalline basement Aquifers, Zimbabwe

Grzybowski M, Lenczewski ME, Oo YY (2019) Water quality and physical hydrogeology of the Amarapura township, Mandalay, Myanmar. Hydrogeol J 27:1497–1513. https://doi.org/10.1007/s.10040-018-01922-9

Hoque M (1984) Pyroclastics from lower benue trough of Nigeria and their tectonic implications. J African Earth Sci 2:351–358

Hossain MT (1981) Geochemistry and petrology of the minor intrusives between Efut Eso and Nko in the Ugep area of Cross River State. J Min Geol 18(1):42–51

Hounslow AW (1995) Water quality data: analysis and interpretation. Lewis, New York

Lee J-Y, Song S-H (2007) Groundwater chemistry and ionic ratios in a western coastal aquifer of Buan, Korea: implications for seawater intrusion. Geosc J 11(3):259–270

Maillet R (1947) The fundamental equations of electrical prospecting. Geophysics 12(4):529–556

Massound U, Santos F, Khalil MA, Taha A, Abbas AM (2010) Estimation of aquifer hydraulic parameters from surface geophysical measurements: a case study of the Upper Cretaceous aquifer, central Sinai. Egypt Hydrogeol J 18:699–710

Mbipom EW, Okon-Umoren OE, Umoh JU (1990) Geophysical investigations of salt ponds in Okpoma area of southeastern Nigeria. J Min Geol 26(2):285–290

Mbonu PDC, Ebeniro JO, Ofoegbu CO, Ekine AS (1991) Geoelectric sounding for the determination of aquifer characteristics in parts of the Umuahia area of Nigeria. Geophysics 5(2):284–291

McDonald AM, Davies J, Peart RJ (2001) Geophysical methods for locating groundwater in low permeability sedimentary rocks: examples from southeast Nigeria. Jour Afric Earth Sci 32(1):115–131

Meybeck M (1987) Global chemical weathering of surficial rocks estimated from river dissolved loads. Am J Sci 287:401–428

Negrel Ph, Petelet-Giraud E, Barbier J, Gautier E (1993) Surface water-groundwater interactions in an alluvial plain: chemical and isotopic systematics. J Hydrol 277:248–267

Niwas S, Singhal DC (1981) Aquifer transmissivity of porous media from resistivity. J Hydrol 82:143–153

Ofoegbu CO (1990) The benue trough: structure and evolution, Informatica International, California

Okamkpa JR, Okonkwo AC, Udejiofor EC, Amoke IA, Aganigbo CI (2018) Groundwater exploration in parts of Enugu east local government area, Enugu state Nigeria. J Nat Sci Res 8(18):32–42

Okereke CS, Esu EO, Edet AE (1998) Determination of potential groundwater sites using geological and geophysical techniques in the Cross RIVER State, southern Nigeria. J African Earth Sci 27(1):149–163

Okonkwo AC, Ezeh CC, Amoke AI (2016) Evaluation of groundwater potential status in Nkanu-West Local Government Area, Enugu State, Nigeria. J Appl Geol Geophys 4(6):79–87

Onuoha KM, Mbazi FCC (1988) Aquifer transmissivity from electrical sounding data: the case of Ajali sandstone aquifers, southeast of Enugu, Nigeria. In: Ofoegbu CO (ed) Groundwater and mineral resources of Nigeria. Vieweg, Braunschweig, Germany, pp 17–29

Onwe IM, Otosigbo GO, Eluwa NN, Nkitnam EE (2019) Geotechnical and hydrochemical assessment of groundwater for potability in Ebonyi North, Southeastern Nigeria. Int J Geol Min 5(1):237–244

Parasnis DS (1986) Principles of applied geophysics, 5th edn. Chapman and Hall, London

Raghunath HM (1987) Groundwater Wiley Eastern Ltd, New Delhi, India

Ravikumar P, Somashekar RK, Angami M (2011) Hydrochemistry and evaluation of groundwater suitability for irrigation and drinking purposes in the Markandeya River basin, Belgium District, Karnataka State India. Environ Monit Assess 173(1–4):459–487

Reddy DV, Nagabhushanam P, Peters E (2011) Village environs as source of nitrate contamination in groundwater: a case study in basaltic geo-environment in central India. Environ Monit Assess 174:481–492

Richards LA (1954) Diagnosis and improvement of saline alkali soils, agriculture 160, Handbook 60. US Department of Agriculture, Washington DC

Rose S (2002) Comparative major ion geochemistry of piedmont streams in the Atlanta, Georgia region: possible effects of urbanization. Environ Geol 42(1):102–113

Sawyer GN, McCarty DL (1967) Chemistry of sanitary engineers, 2nd edn. McGraw Hill, New York

Singh AK, Raj B, Tiwari AK, Mahato MK (2013) Evaluation of hydrochemical processes and groundwater quality in the Jhansi district of Bundelkhand region. Environ Earth Sci, India. https://doi.org/10.1007/s12665-012-2209-7

Stallard RF, Edmond JM (1983) Geochemistry of the Amazon: 2. the influence of geology and weathering environment on the dissolved load. J Geophys Res Oceans 88:9671–9688

Telford WM, Geldart LP, Sheriff RE, Keys DA (1978) Applied geophysics. Cambridge University Press, New York

Tijani MN, Löehnert EP, Uma KO (1996) Origin of saline groundwaters in Ogoja area, Lower Benue Trough. Nigeria J Afric Earth Sci 23(2):237–252

Tizro AT, Voudouris KS, Salehzade M, Mashayekhi H (2010) Hydrogeological framework and estimation of aquifer hydraulic parameters using geoelectrical data: a case study from West Iran. Hydrogeol J 18(4):917–929

Ukpai SN, Okogbue CO (2017) Geophysical, geochemical and hydrological analyses of water-resource vulnerability to salinization: case of Uburu-Okposi salt lakes and environs, southeast Nigeria. Hydrogeol J 25:1997–2014

Uma KO, Onuoha KM (1990) Groundwater resources of the lower benue trough. In benue trough: structure and evolution (edn Charles Ofoegbu) Friedr. Vieweg & Sohn Braunschweig/Wiesbaden pp 77–91

Uma KO, Onuoha KM, Egboka BCE (1990) Hydrochemical facies, groundwater flow pattern and origin of saline waters in parts of the western flank of the Cross River basin, Nigeria. The Evolution of the Benue Basin (Eds COfoegbu), pp 115–134

Uma O, Lohnert EP (1992) Research on the saline groundwaters in Benue Trough, Nigeria: Preliminary results and projections. Zbl Geol Palaont I Stuttgart 11:2751–2756

Umar ND, Igwe O (2019) Geo-electric method applied to groundwater protection of a granular sandstone aquifer. Appl Water Sci 9:112. https://doi.org/10.1007/s13201-019-0980-2

Umeh VO, Ezeh CC, Okonkwo AC (2014) Groundwater exploration of Lokpaukwu, Abia State, Southern Nigeria, using electrical resistivity method. Int Res J Geol Min 4(3):76–83

Ushie FA, Nwankwoala HO (2011) A preliminary geoelectrical appraisal for groundwater in Yalla, Southern Benue Trough, Southeast Nigeria. Middle-East J Sci Res 9(1):1–7

Vinograd N, Porowski A (2020) Application of isotopic and geochemical studies to explain the origin and formation of mineral waters of Staraya Russa Spa. NW Russia Environ Earth Sci 79:183. https://doi.org/10.1007/s12665-020-08923-6

WHO (2011) Guidelines for drinking-water quality, 4th edn. World Health Organization, Geneva

Wilcox LV (1955) Classification and use of irrigation waters US Department of agriculture circular, pp 969

Zhang J, Huang WW, Letolle R, Jusserand C (1995) Major element chemistry of the Huanghe (Yellow river), China-weathering processes and chemical fluxes. J Hydrol 168:173–203

Zohdy AAR, Eaton GP, Mabey DR (1974) Application of surface geophysics to groundwater investigation. United States Geological Survey Book 2, Chapter D1, pp 116